

NOAA Technical Memorandum NESDIS 20



**SATELLITE OBSERVED MESOSCALE CONVECTIVE
SYSTEM (MCS) PROPAGATION CHARACTERISTICS
AND A 3-12 HOUR HEAVY PRECIPITATION
FORECAST INDEX**

Washington, D.C.

December 1987

UNITED STATES
DEPARTMENT OF COMMERCE

National Oceanic and
Atmospheric Administration

National Environmental Satellite,
Data, and Information Service

NOAA TECHNICAL MEMORANDUMS

National Environmental Satellite, Data, and Information Service

The National Environmental Satellite, Data, and Information Service (NESDIS) manages the Nation's civil Earth-observing satellite systems, as well as global national data bases for meteorology, oceanography, geophysics, and solar-terrestrial sciences. From these sources, it develops and disseminates environmental data and information products critical to the protection of life and property, national defense, the national economy, energy development and distribution, global food supplies, and the development of natural resources.

Publication in the NOAA Technical Memorandum series does not preclude later publication in scientific journals in expanded or modified form. The NESDIS series of NOAA Technical Memorandums is a continuation of the former NESS and EDIS series of NOAA Technical Memorandums and the NESC and EDS series of the Environmental Science Services Administration (ESSA) Technical Memorandums.

These memorandums are available from the National Technical Information Service (NTIS), U.S. Department of Commerce, Sills Bldg., 5285 Port Royal, Springfield, VA 22161 (prices on request for paper copies or microfiche, please refer to PB number when ordering) or by contacting Nancy Everson, NOAA/NESDIS, 5200 Auth Road, Washington, DC 20233 (when extra copies are available). A partial listing of more recent memorandums appear below:

- NESS 113 Satellite Identification of Surface Radiant Temperature Fields of Subpixel Resolution. Jeff Dozier, December 1980. (PB81 184038)
- NESS 114 An Attitude Predictor/Target Selector. Bruce M. Sharts, February 1981. (PB81 200479)
- NESS 115 Publications and Final Reports on Contracts and Grants, 1980. Nancy Everson, June 1981. (PB82 103219)
- NESS 116 Modified Version of the TIROS N/NOAA A-G Satellite Series (NOAA E-J) - Advanced TIROS-N (TN). Arthur Schwalb, February 1982. (PB82 194044)
- NESS 117 Publications and Final Reports on Contracts and Grants, 1981. Nancy Everson, April 1982. (PB82 229204)
- NESS 118 Satellite Observation of Great Lakes Ice - Winter 1979-80. Sharolyn Reed Young, July 1983. (PB84 101054)
- NESS 119 Satellite Observation of Great Lakes Ice: 1980-81. A.L. Bell, December 1982. (PB83 156877)
- NESDIS 1 Publications and Final Reports on Contracts and Grants, 1982. Nancy Everson, March 1983. (PB83 252528)
- NESDIS 2 The Geostationary Operational Environmental Satellite Data Collection System. D.H. MacCallum and M.J. Nestlebusch, June 1983. (PB83 257634)
- NESDIS 3 Nimbus-7 ERB Sub-Target Radiance Tape (STRT) Data Base. L.L. Stowe and M.D. Fromm, November 1983. (PB84 149921)
- NESDIS 4 Publications and Final Reports on Contracts and Grants, 1983. Nancy Everson, April 1984. (PB84 192301)
- NESDIS 5 A Tropical Cyclone Precipitation Estimation Technique Using Geostationary Satellite Data. Leroy E. Spayd Jr. and Roderick A. Scofield, July 1984. (PB84 226703)
- NESDIS 6 The Advantages of Sounding with the Smaller Detectors of the VISSR Atmospheric Sounder. W. Paul Menzel, Thomas H. Achtor, Christopher M. Hayden and William L. Smith, July 1984. (PB851518/AS)
- NESDIS 7 Surface Soil Moisture Measurements of the White Sands, New Mexico. G.R. Smith, September 1984. (PB85 135754)

NOAA Technical Memorandum NESDIS 20

**SATELLITE OBSERVED MESOSCALE CONVECTIVE
SYSTEM (MCS) PROPAGATION CHARACTERISTICS
AND A 3-12 HOUR HEAVY PRECIPITATION
FORECAST INDEX**

Jiang Shi
Satellite Meteorological Center
Beijing, People's Republic of China

and

Roderick A. Scofield
Satellite Applications Laboratory
Washington, D.C.

December 1987

UNITED STATES
DEPARTMENT OF COMMERCE
C. William Verity, Secretary

National Oceanic and
Atmospheric Administration
J. Curtis Mack, II,
Acting Under Secretary

National Environmental Satellite,
Data, and Information Service
Thomas N. Pyke,
Assistant Administrator



CONTENTS

	<u>Page</u>
Abstract.....	
I. Introduction.....	1
II. Review of Conventional Thunderstorm Propagation Concepts.....	5
III. Mesoscale Convective System (MCS) Propagation Characteristics in 30 Minute Interval Satellite Imagery.....	7
IV. An Example of a Forward and Backward Propagating MCS.....	15
V. A Short Range Forecasting Technique for Expected Storm Propagation.....	19
VI. Life Cycle Characteristics of MCSs.....	27
VII. A Proposed 3-12 Hour Heavy Precipitation Forecast Index.....	32
VIII. Summary and Outlook.....	40
IX. Acknowledgments.....	41
X. References.....	41

SATELLITE OBSERVED MESOSCALE CONVECTIVE SYSTEM (MCS) PROPAGATION
CHARACTERISTICS AND A 3-12 HOUR HEAVY PRECIPITATION FORECAST INDEX

Jiang Shi
Satellite Meteorological Center
Beijing, People's Republic of China

and

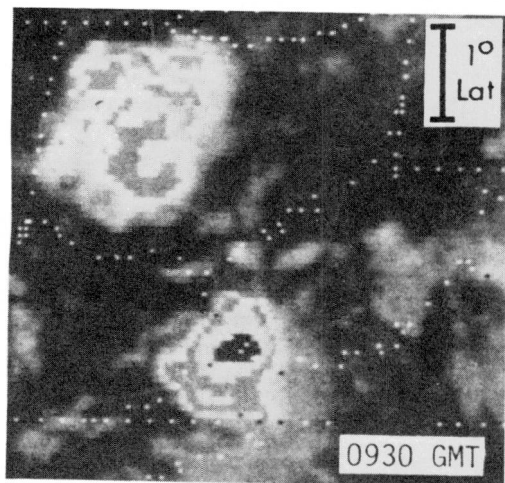
Roderick A. Scofield
Satellite Applications Laboratory
Washington, DC

ABSTRACT. One of the greatest challenges of an operational meteorologist is predicting the direction and speed of movement of Mesoscale Convective Systems (MCS). In most cases, propagation is the controlling influence on the movement of MCSs. The type of propagation (backward or forward) often determines the amount of rainfall that occurs from a MCS. This memorandum briefly discusses previous concepts on thunderstorm propagation. Discussion and pertinent examples of MCS propagation characteristics observed in the GOES satellite imagery are presented. Two types of satellite propagation characteristics are identified. A short range forecasting technique for expected storm propagation is described. Finally, a preliminary 3-12 hour heavy precipitation forecast index for MCSs is presented.

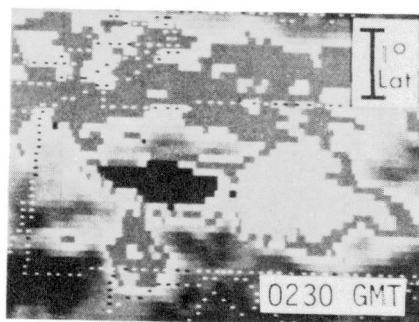
I. INTRODUCTION

Convective systems observed in the satellite imagery often have unique cloud patterns and/or cloud top temperature characteristics. As a result, satellite observed convective cloud categories associated with heavy precipitation, have been identified and discussed in previous papers (see Scofield, 1985 and Fleming and Spayd, 1986). Those categories are displayed in Figures 1a and 1b; spatial and temporal scales are provided in Figure 1c. The emphasis in this paper is on cold-topped (colder than -62°C) Mesoscale Convective Systems (MCS). Synoptic-scale tropical, Mesoscale Convective Complex (MCC) (Maddox, 1980), multi-clustered linear and multi-clustered circular systems, shown in Figure 1a are examples of MCSs.

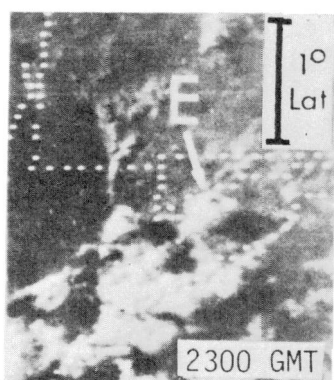
One of the greatest challenges of an operational meteorologist is predicting when a MCS will become quasi-stationary or even move backward. These peculiar behaviors often result in flash floods. The controlling influence on the movement and speed of MCSs is the propagation effect. Since there is a relationship between storm propagation and rainfall amount, research on MCS propagation is extremely important. This paper will show that storm propagation observed in the 30 minute interval GOES satellite imagery is somewhat different from the propagation discussed by Chappell (1985), Doswell (1985), Merritt and Fritsch (1984) and others.



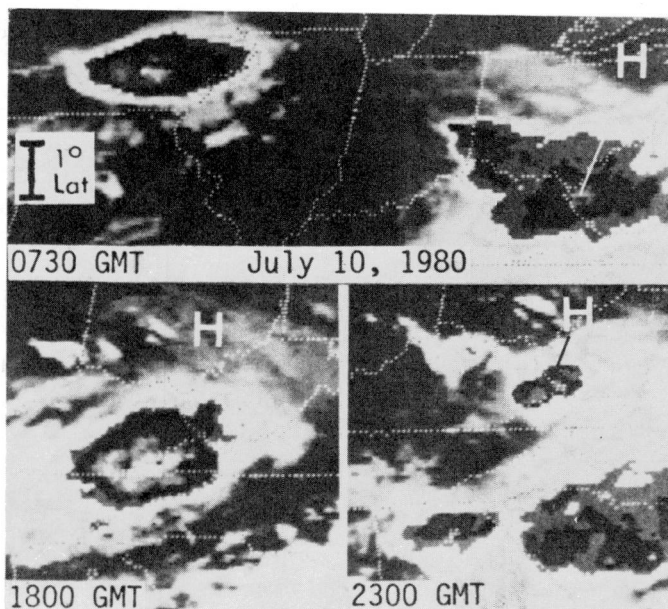
Multi-Clustered Circular



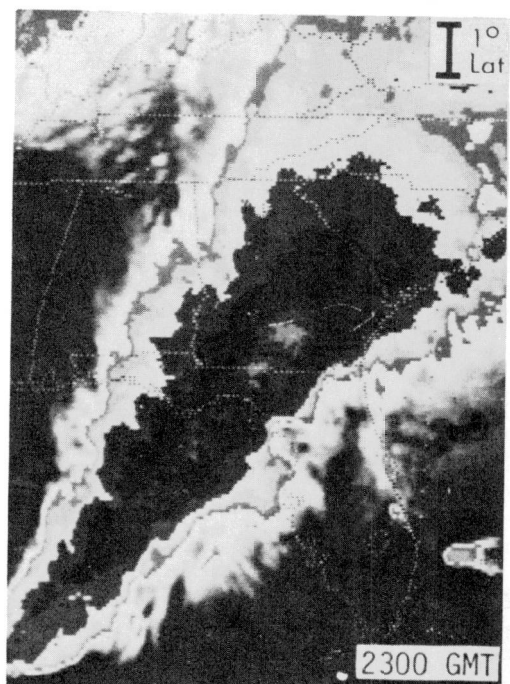
Multi-Clustered Linear



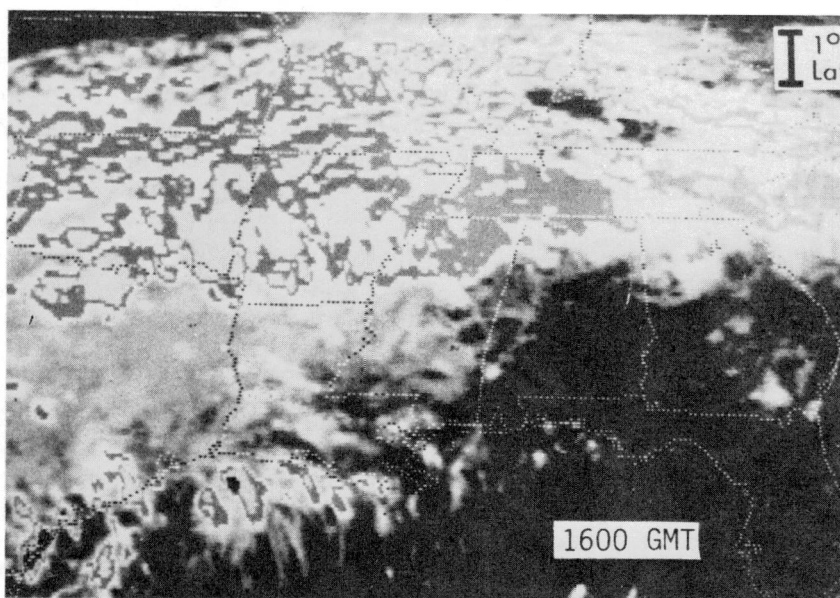
Single-Clustered



Combination

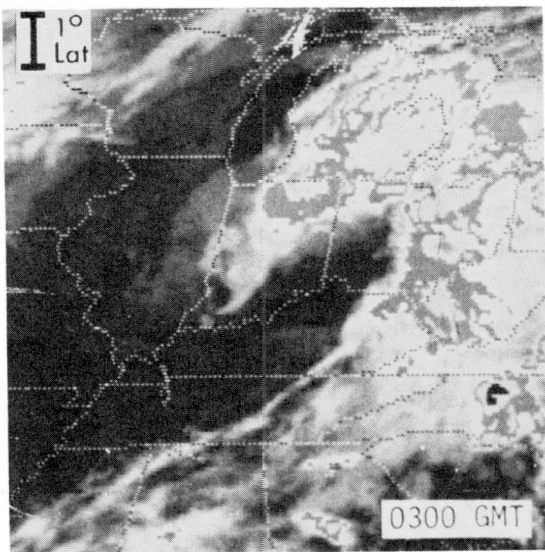


Squall Line

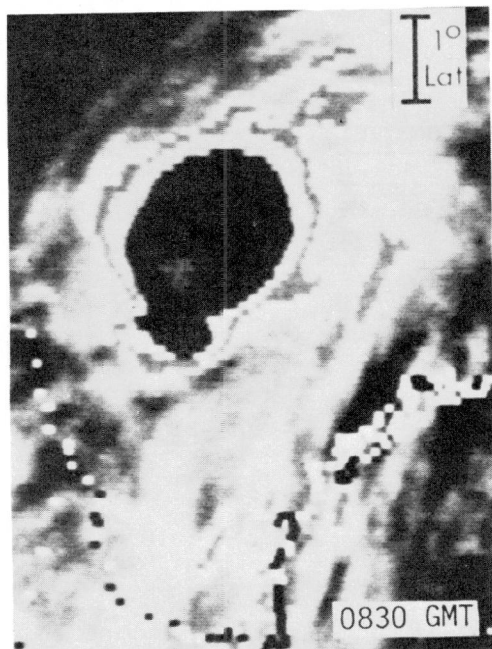


Large-Scale Overrunning

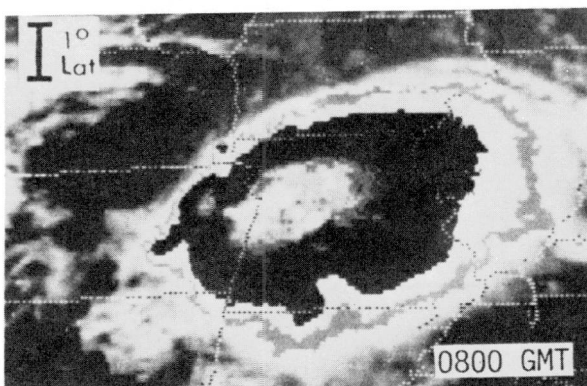
Figure 1a. Types of heavy precipitation producing convective systems.



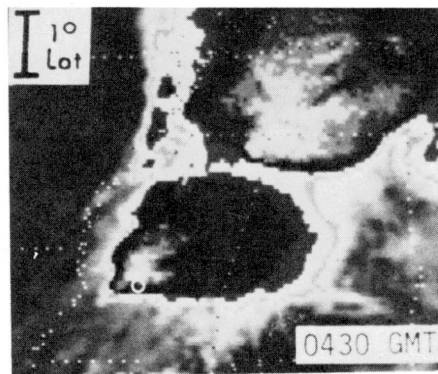
Synoptic-Scale
Cyclonic Circulation



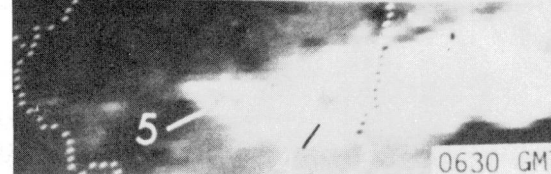
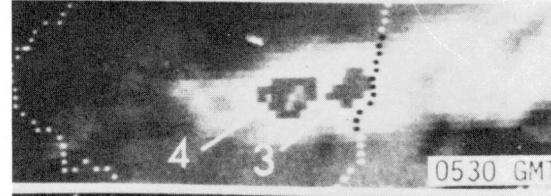
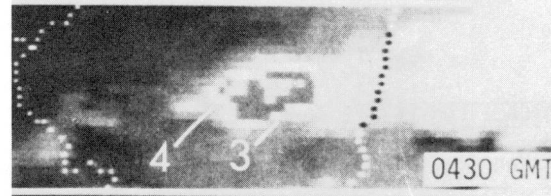
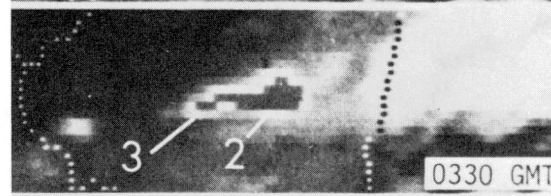
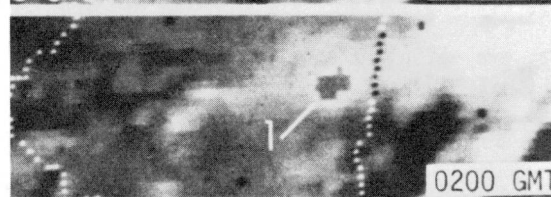
Synoptic-Scale Tropical



Mesoscale Convective Complex



Large-Scale Wedge



Regenerative

Figure 1b. Types of heavy precipitation producing convective systems.

SCALES OF SATELLITE-OBSERVED HEAVY CONVECTIVE RAINFALL SYSTEMS

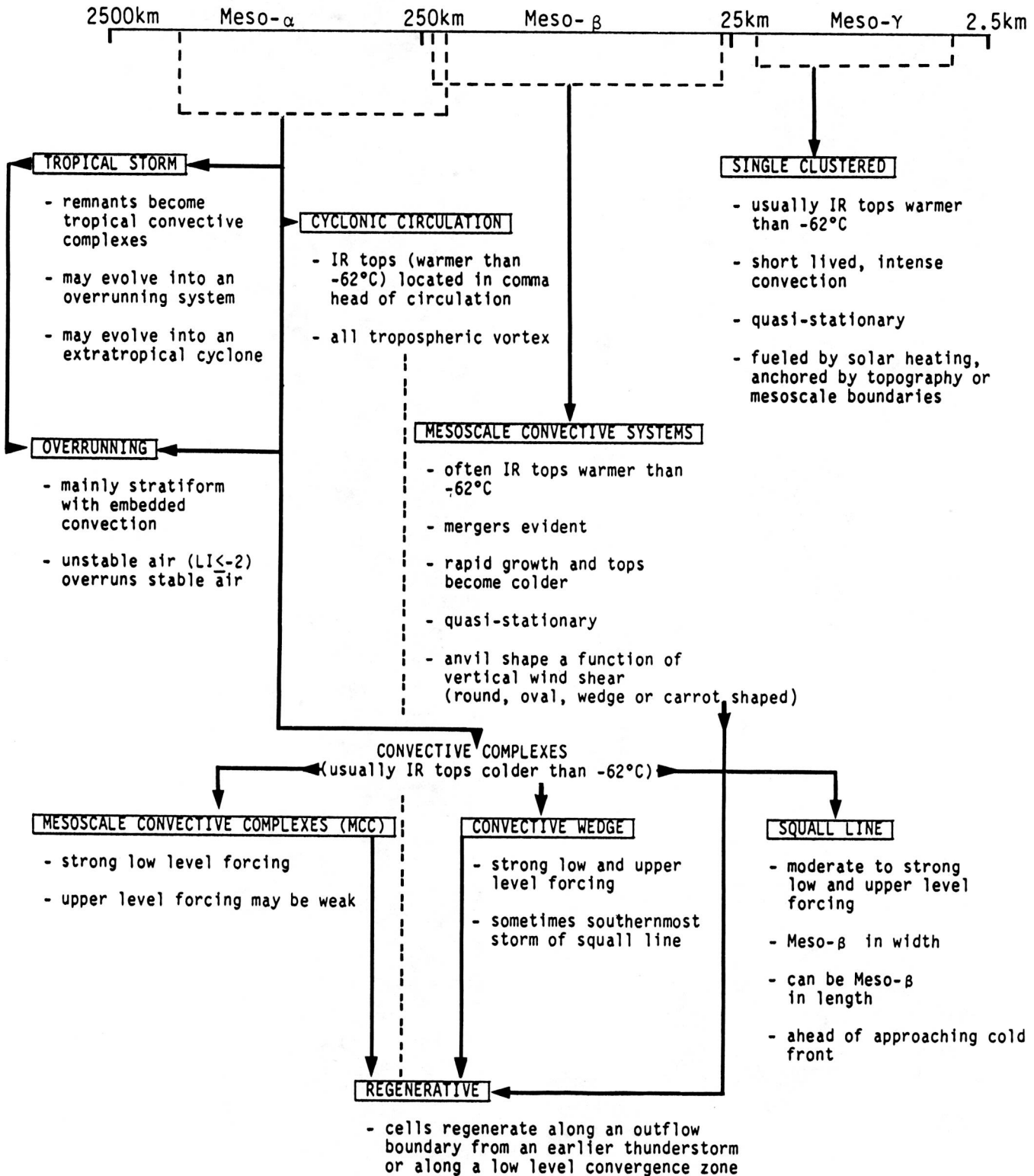


Figure 1c. Scales of satellite-observed heavy convective rainfall systems.

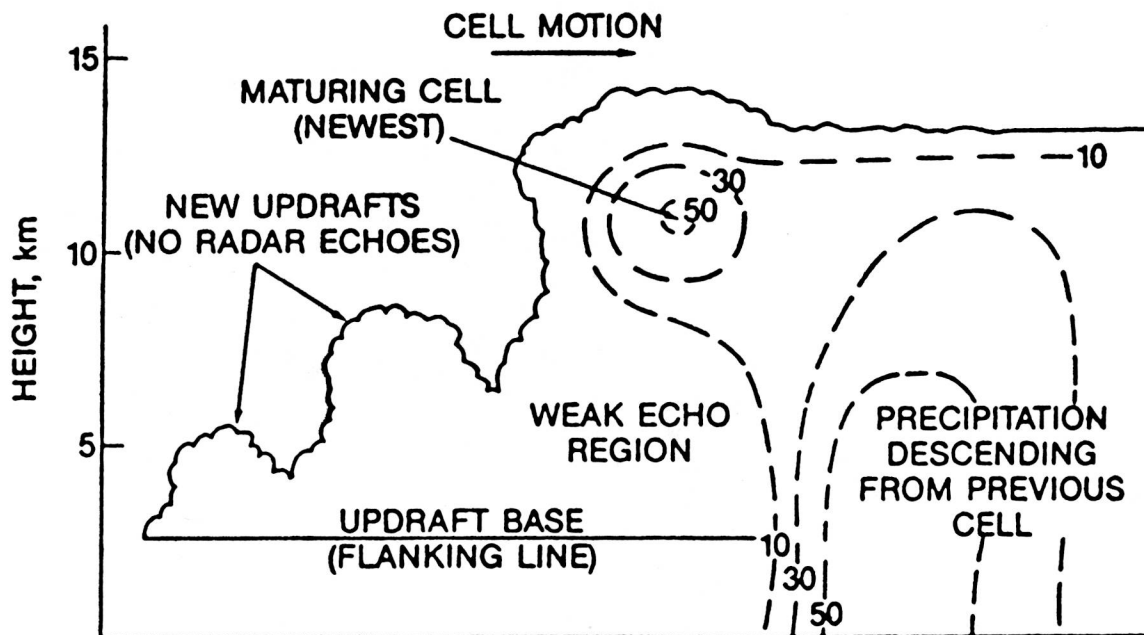


Figure 2. A schematic of thunderstorm propagation with cells, forming on the left and moving from left to right, creating a multicell thunderstorm complex. Dashed lines represent radar reflections of 10, 30 and 50 dBZ (from Doswell, 1985).

II. REVIEW OF CONVENTIONAL THUNDERSTORM PROPAGATION CONCEPTS

Propagation refers to the movement of thunderstorms as a result of preferred new cell development on one flank (usually on the right or right rear) of the updraft. Propagation occurs because of the storm's interactions with an environment possessing potential buoyant energy and moisture convergence. Propagation results in new convective cells being formed on the flank of the storm and accreting (growing by being added to) to the periphery of the storm; this produces either a continuous or discrete movement of the most active part of the storm.

Doswell's (1985) schematic model of storm propagation is shown in Figure 2. In this schematic, new cells develop and grow taller as they approach and finally merge with the maturing cell. These new merging cells eventually become the dominant cells of the MCS. Chappell (1985) asserts that the younger towering cumulus do not have precipitation. Eventually, precipitation forms in the updraft and is held aloft temporarily while the cell matures. Finally, the mature cell unloads the precipitation as a heavy gush or burst of rain.

The orientation of the propagation can be approximated by assessing which storm flank intercepts moist, low level, conditionally unstable air (Merritt and Fritsch, 1984). The magnitude of the propagation depends on the rate at which new cells form, the separation distance between the newly developed cell and the existing storm and the rate at which the new cell enlarges and accretes to the storm boundary. New cells would be expected to form along a particular segment of a frontal boundary (or outflow boundary). That segment (see Figure 3) may be identified by the juxtaposition of the low level thermal axis, the low level jet, the moist tongue and the higher gradient of instability (Chappell, 1985 and Scofield and Jiang, 1987).

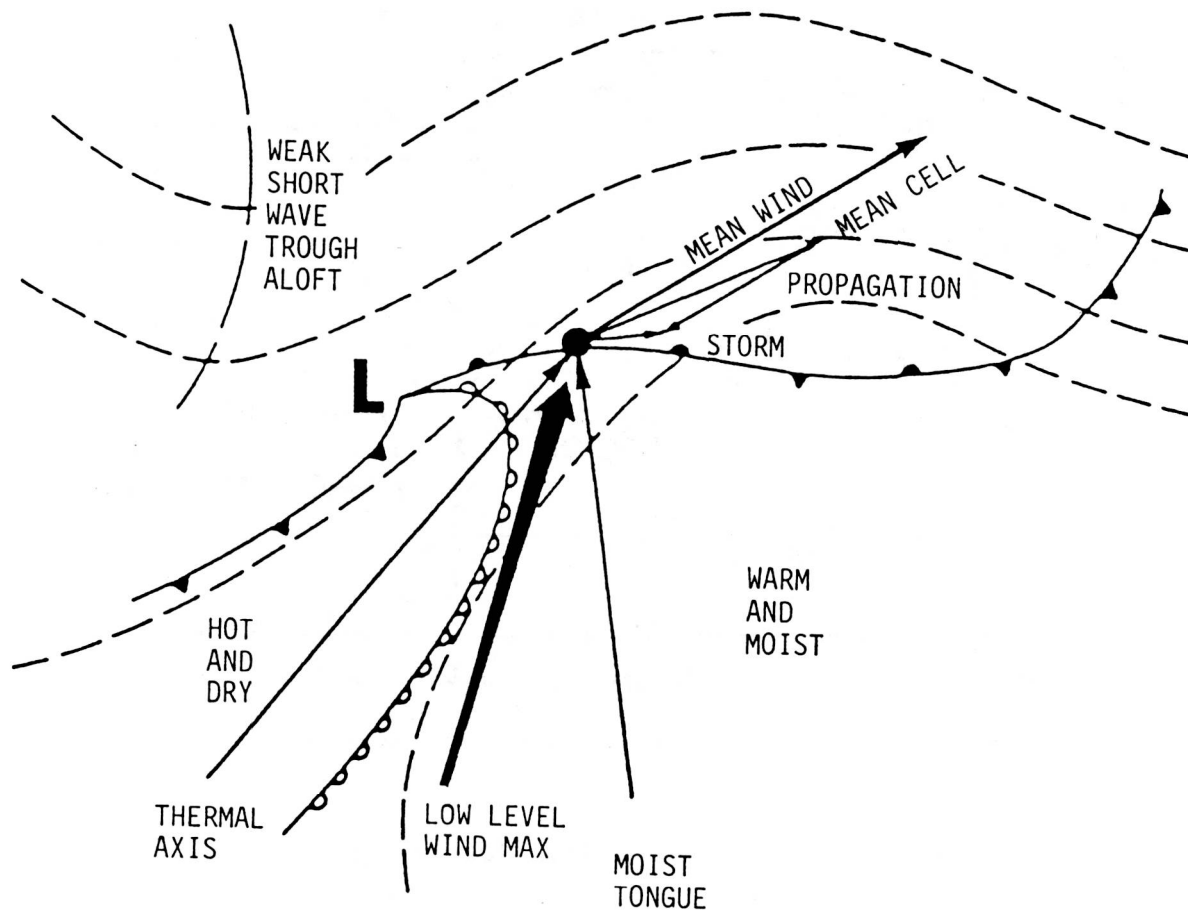


Figure 3. Meteorological conditions that can lead to the formation of a frontal-type, quasi-stationary convective rainstorm (from Chappell, 1985).

There are two types of conventional thunderstorm propagations.

1. Continuous Propagation (Browning, 1964)

In this type of propagation, newly formed cells and their associated updrafts continuously feed the main updraft of the existing storm, rather than providing for the growth of new cells. As a result, these storms propagate continuously.

2. Discrete Propagation (Newton and Newton, 1959)

This type of propagation involves the development of new cells produced from enhanced convergence in the boundary layer; downdrafts from the main storm create the enhanced convergence. New cells typically form 4-10 km away from the main storm and then merge with the main storm; the mergers usually produce an increase in the storm area. Discrete propagation occurs in a series of separate steps; each step is associated with new cell formation (Newton and Fankhauser, 1975). Discrete propagation can significantly effect storm motion, usually causing the storm complex to move to the right of individual cells. The individual cells are observed to move with the mean wind in the convective layer (Brooks, 1946, Wilhelmson and Chen, 1982, Newton and Newton, 1959 and others).

Generally conventional propagation (continuous and discrete) is best detected by high spatial and time resolution radar. An example of discrete propagation in the radar pictures is shown in Figures 4a, 4b, and 4c (Chappell, 1986). In the radar imagery, thunderstorm cells develop back to the west (backward propagation) where very unstable air is overrunning a stationary front and cool dome left from previous thunderstorm activity. This backward propagation produces a rapid generation of new storms that continue for several hours on the west flank of the MCS; flash flooding occurs as storms move repeatedly over the same region.

III. MCS PROPAGATION CHARACTERISTICS IN 30 MINUTE INTERVAL SATELLITE IMAGERY

Some types of propagation observed in the satellite imagery are associated with heavy rain producing MCSs. However, MCS propagation in the satellite imagery cannot be discerned as meticulously as in the higher resolution (both space and time) radar data. Nevertheless, towering cumulus, outflow boundaries and other features important to propagation dynamics are readily observable in the satellite imagery but are not detectable in the radar data.

Satellite-observed storm propagation refers to the translation of the most convective portion or periphery of the MCSs due to the formation and development of regenerative cells. Satellite-observed storm propagation has one or more of the following characteristics:

- (1) Newly formed cells appear to continuously feed the main MCS; this is similar to the conventional type of continuous propagation.
- (2) A series of regenerating cells form and grow near the periphery of the main MCS and finally merge with the MCS; this is similar to the conventional type of discrete propagation.

and

- (3) Two or more independent MCSs merge together forming an intense area of convection; this occurs when one MCS exhibits forward propagation and the other MCS propagates backwards resulting in a merger of the two systems.

Though there are similarities, propagation determined from satellite pictures is different from the conventional and radar propagation discussed in Section II. Analysis of 36 events indicates that two types of MCS satellite propagation characteristics are observed.

TYPE I: CONTINUOUS PROPAGATION

TYPE II: BOUNDED PROPAGATION

All propagation events deviated from the mean wind direction. The continuous type of conventional propagation belongs to the satellite Type I. In some discrete types of conventional propagations, the new convective systems developed near the periphery of the main MCS; a merger then occurs between these two systems. The merger happens so quickly (in less than 30 minutes) that the

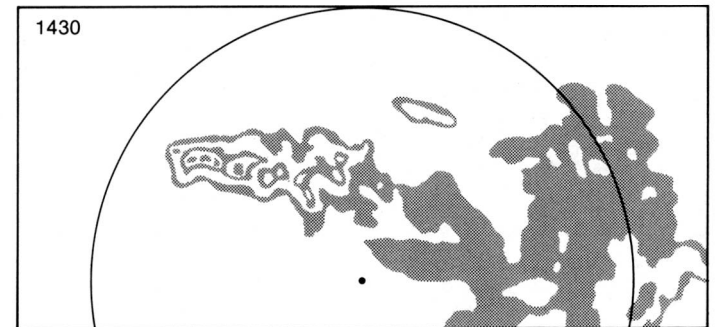
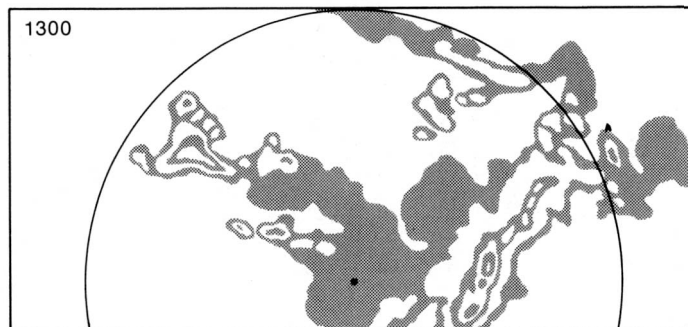
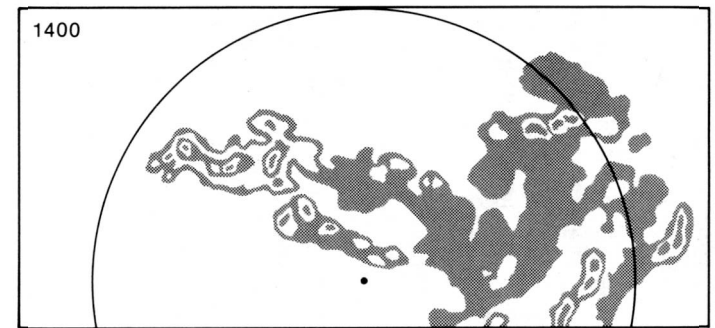
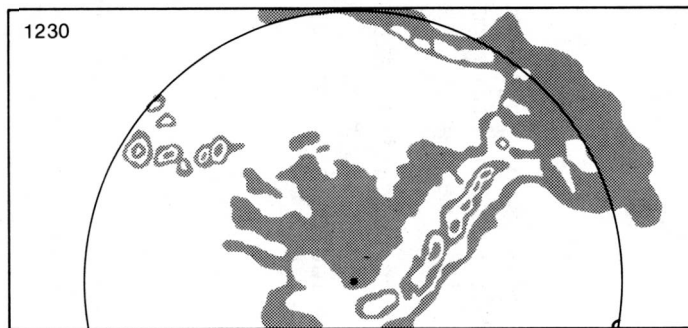
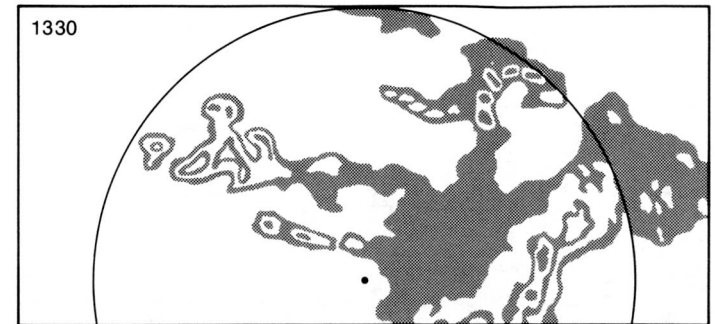
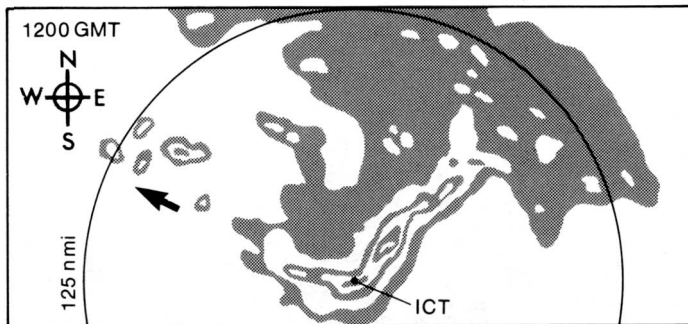


Figure 4a. A radar example of backward discrete propagation is indicated by arrow. Wichita (ICT) radar depictions of central Kansas quasi-stationary rainstorm, June 22, 1981. All radar VIP intensity levels are shown, beginning with gray for level one and alternating white and gray for higher levels. Times are GMT (from Chappell, 1986).

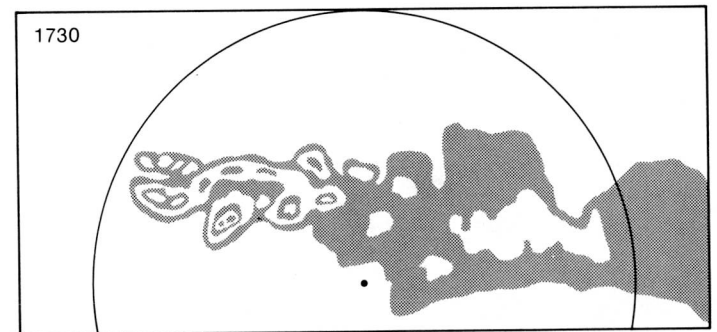
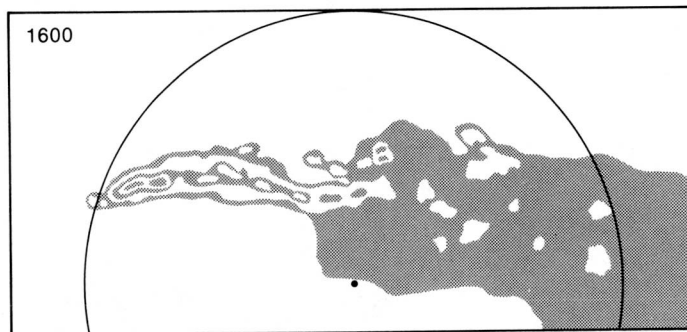
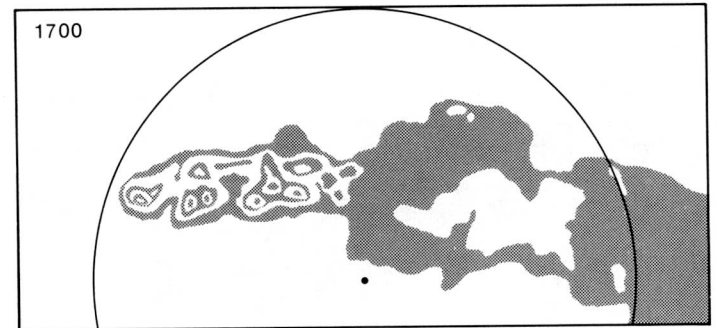
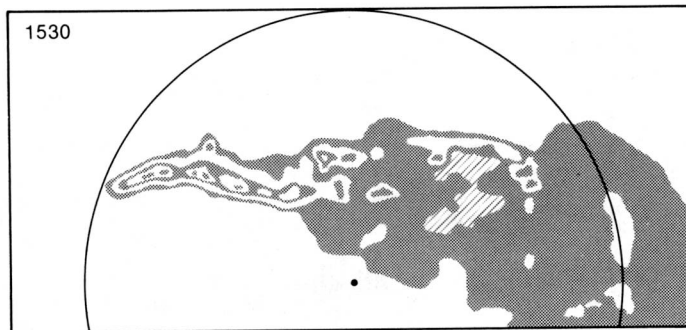
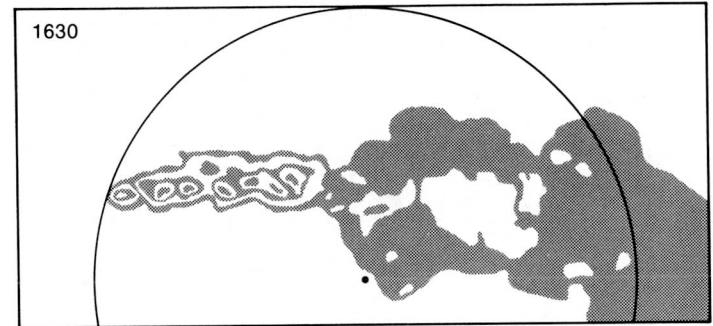
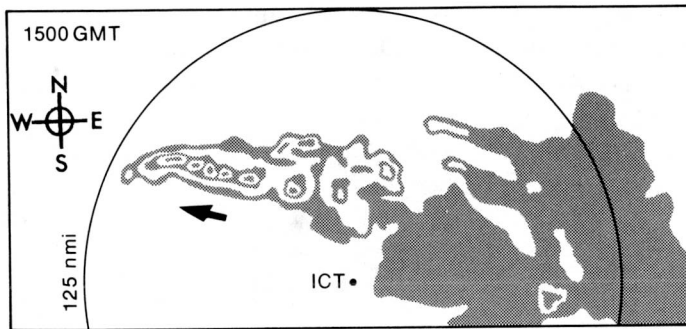


Figure 4b. A radar example of backward discrete propagation is indicated by arrow. Wichita (ICT) radar depictions of central Kansas quasi-stationary rainstorm, June 22, 1981. All radar VIP intensity levels are shown, beginning with gray for level one and alternating white and gray for higher levels. Times are GMT (from Chappell, 1986).

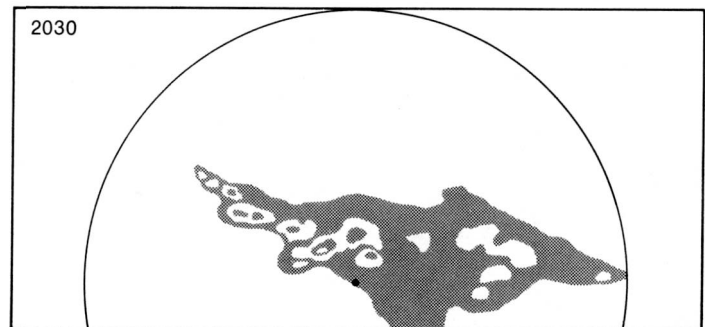
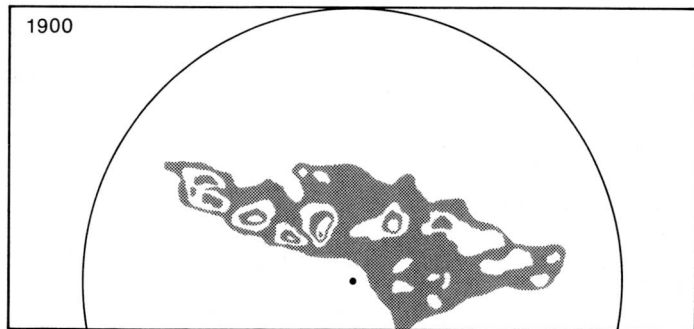
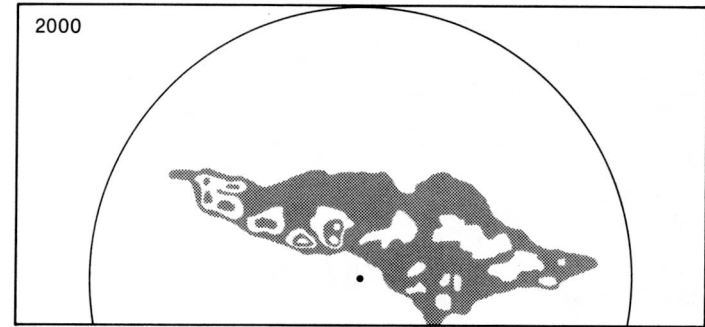
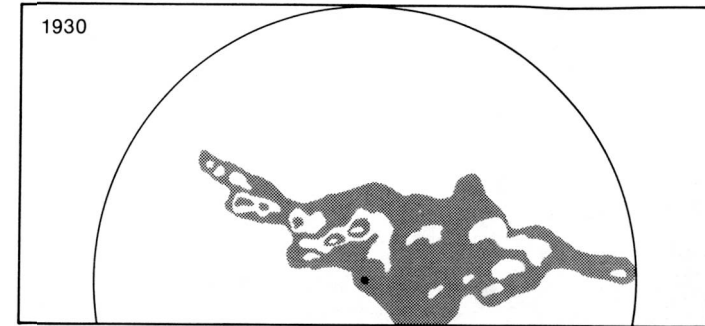
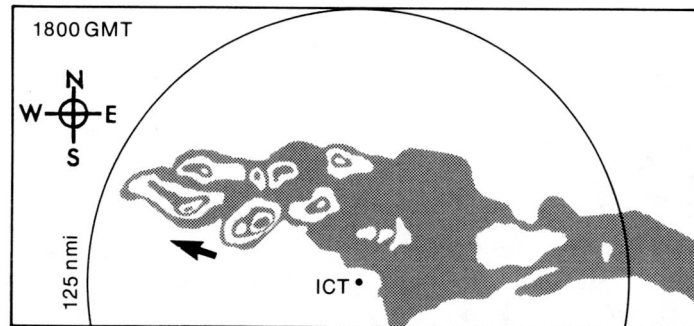


Figure 4c. A radar example of backward discrete propagation is indicated by arrow. Wichita (ICT) radar depictions of central Kansas quasi-stationary rainstorm, June 22, 1981. All radar VIP intensity levels are shown, beginning with gray for level one and alternating white and gray for higher levels. Times are GMT (from Chappell, 1986).

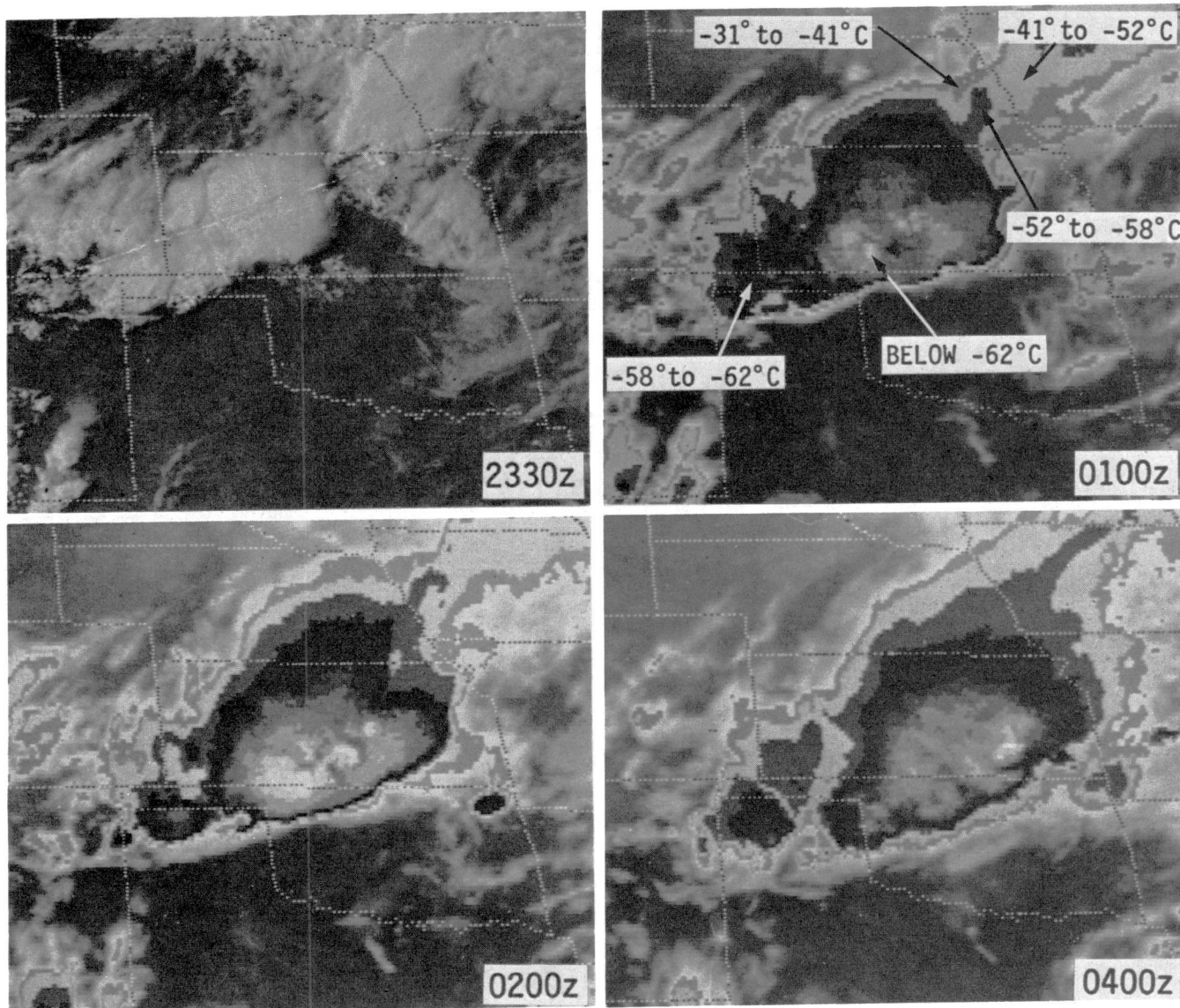


Figure 5. An example of a continuous MCS propagation (Type I); also classified as a right mover or forward propagating MCS. VIS imagery (2330 GMT) June 10, 1985 and enhanced IR imagery (MB Curve), June 11, 1985.

periphery of the storm appears to move continuously in the satellite pictures. Therefore, this kind of discrete propagation belongs to Type I. Type I propagation is often best detected by radar data and high resolution visible (VIS) satellite imagery - an example of a continuous propagating storm is shown in Figure 5; this storm would be classified as a right mover or forward propagating storm. Right mover (or left mover) refers to the deviation of the storm's movement from the mean tropospheric wind. Forward propagating storms are ones that have an eastward component (NE, E or SE) of movement; backward propagation refers to a westward (NW, W or SW) component of movement.

Type II occurs when the periphery of the storm in the satellite picture is clearly bounded (separated) from any other convective system. In this situation, the main MCS merges with another, much smaller and separate convective system. Often these smaller convective systems (sometimes towering cumuli) have been "triggered" by an outflow boundary produced earlier by the main MCS. The outflow boundary can be 20 km or more from the main MCS. An example of a

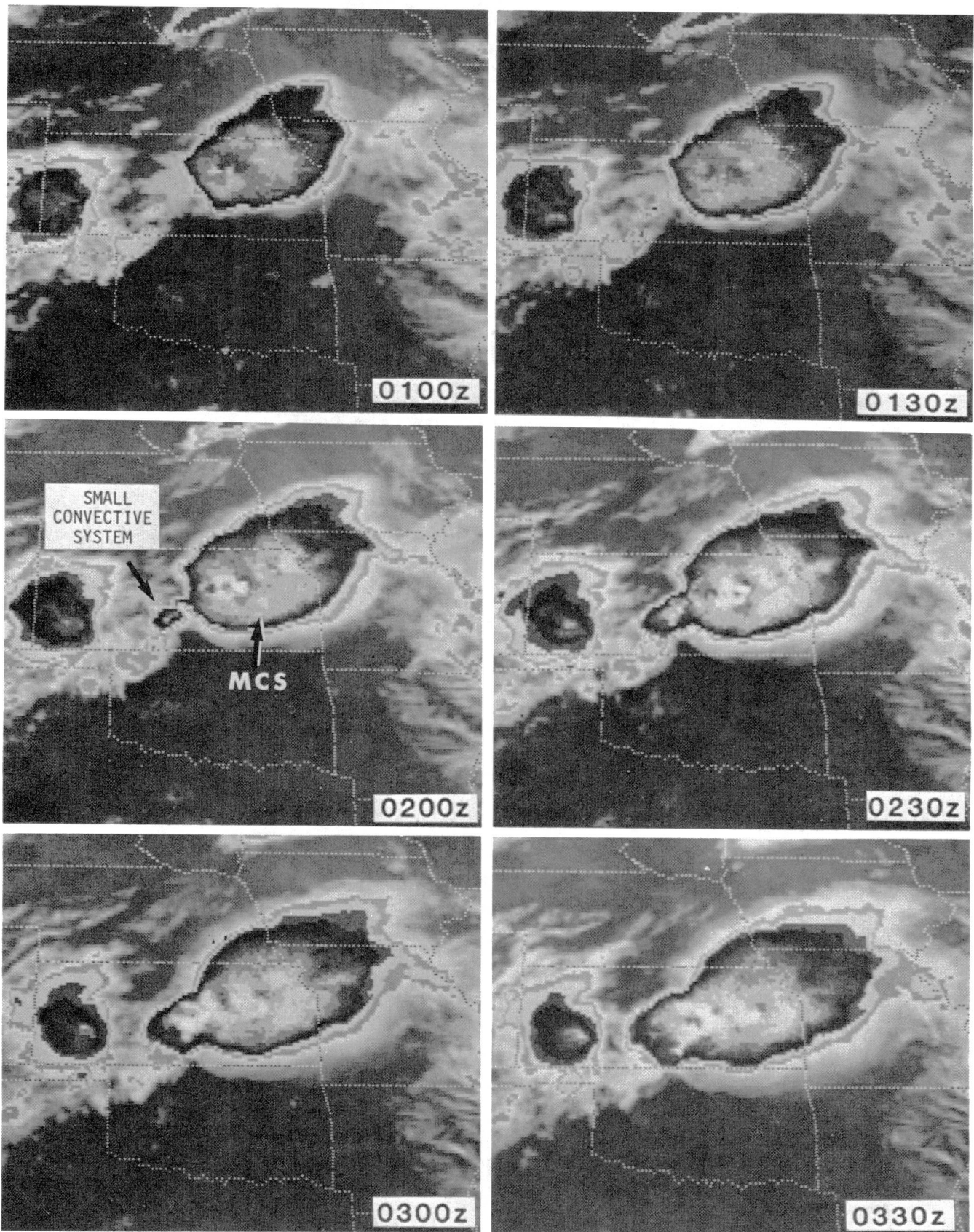


Figure 6. An example of a bounded MCS propagation (Type II); also classified as an opposite (back) mover or backward propagating MCS. Enhanced IR imagery (MB Curve), August 4, 1985.

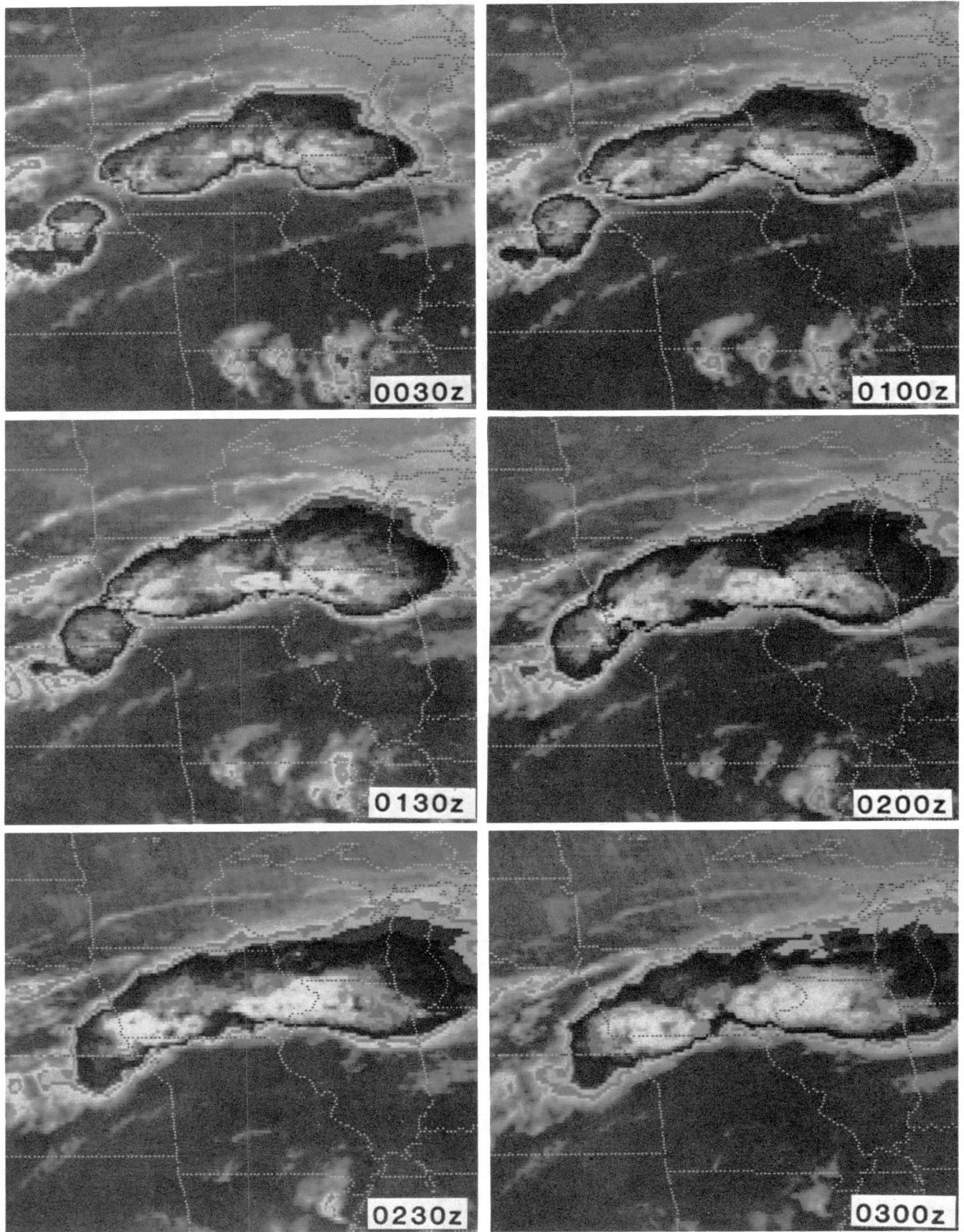


Figure 7. An example of a bounded MCS propagating (Type II); the merger of two independent MCSs. Enhanced IR imagery (MB Curve), July 9, 1986.

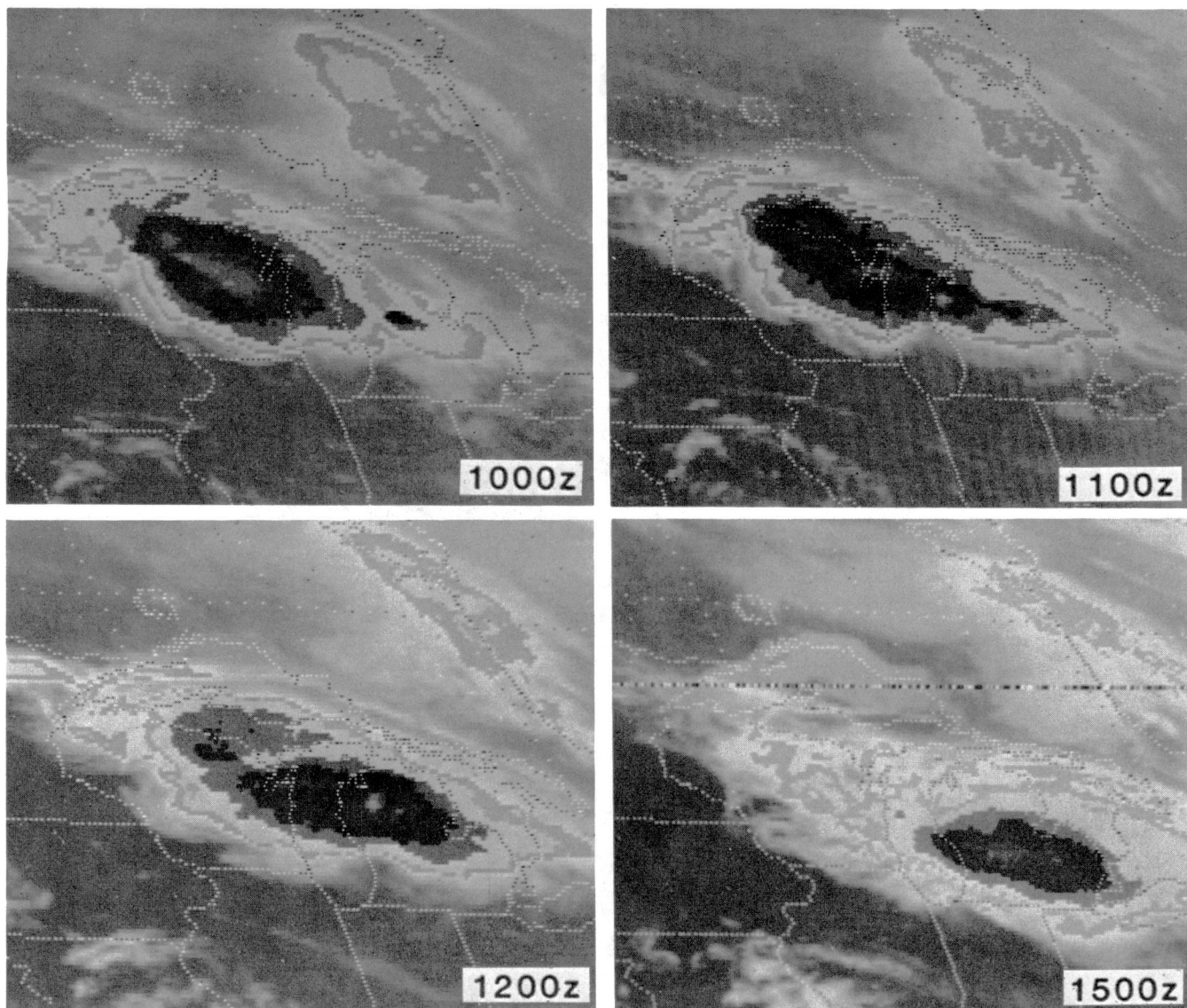


Figure 8a. A forward propagating MCS; enhanced IR imagery (MB Curve), June 19, 1986.

bounded propagation is depicted in Figure 6; this storm is propagating backwards to the southwest. An example of a bounded propagation characterized by the merger of two or more independent MCSs is shown in Figure 7. The MCS over southwestern Iowa produced 4 to 8 inches of rain and flash floods. Sometimes negative hourly surface pressure tendencies occur between two MCSs that are going to merge; positive tendencies are observed between MCSs that do not merge. In some cases bounded propagation (Type II) is quite similar to continuous propagation (Type I). This similarity occurs because newly formed cells can develop close to the main MCS (10 to 20 km) and then merge quite rapidly with the main MCS.

Forward or backward moving MCSs can be either Type I or Type II propagations. However, backward movers appear to be more frequently associated with Type IIs. The relationships between conventional and satellite propagation are summarized in Table 1.

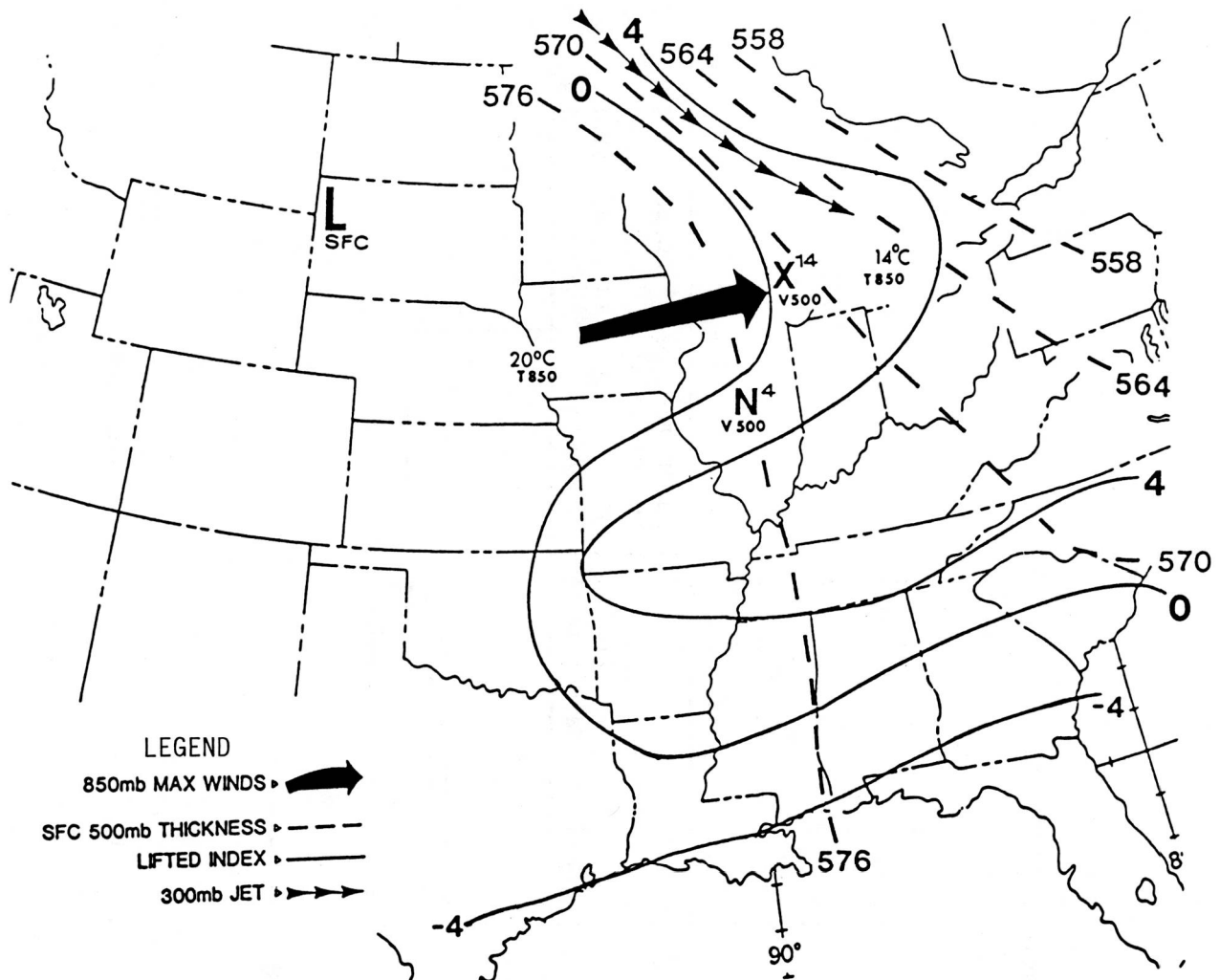


Figure 8b. Surface and upper air features for June 19, 1981, 1200 GMT; T₈₅₀ indicates 850 mb temperatures in that area and V₅₀₀ locates either a 500 mb maximum vorticity center (X) or a minimum vorticity center (N). Vorticity values are indicated in 10^{-5} sec^{-1} . L_{sfc} locates a surface low pressure area.

IV. AN EXAMPLE OF A FORWARD AND BACKWARD PROPAGATION MCS

Forward Propagating MCS (June 19, 1986)

An example of a forward propagating MCS is shown in Figures 8a. Important surface and upper air features are shown in Figure 8b. As the MCS moves south-eastward, colder tops (1100 and 1200 GMT) are observed in the southeastern portion of the system; this feature is typical of forward propagating systems. In addition to the rapid forward (southeast) propagation of the MCS from northern Wisconsin to central Michigan, other features noted are an east-west quasi-stationary front from northern Michigan to Wyoming (not analyzed in Figure 8b), a 850 mb flow maintaining unstable air to the leading edge of the MCS, a positive vorticity advection (PVA) center, northwest-southeast thickness isopleths with a moderate gradient and a strong upper level flow pattern. Observed rainfall with this MCS ranged from 1-2 inches; there were isolated maxima of 3 to 4 inches. Many instances of "straight line" wind damage were reported.

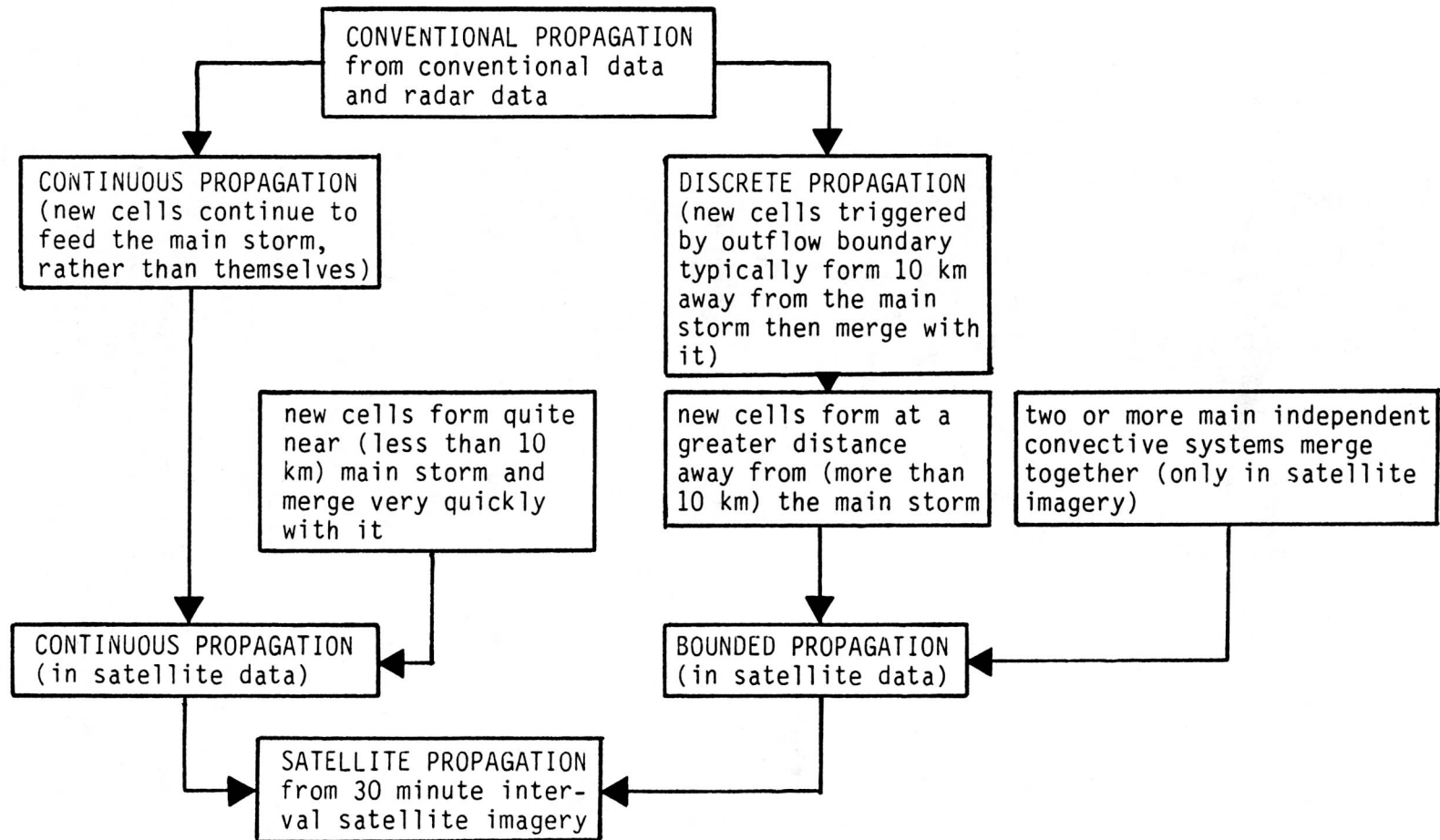


Table 1. The relationship between conventional propagation and satellite propagation.

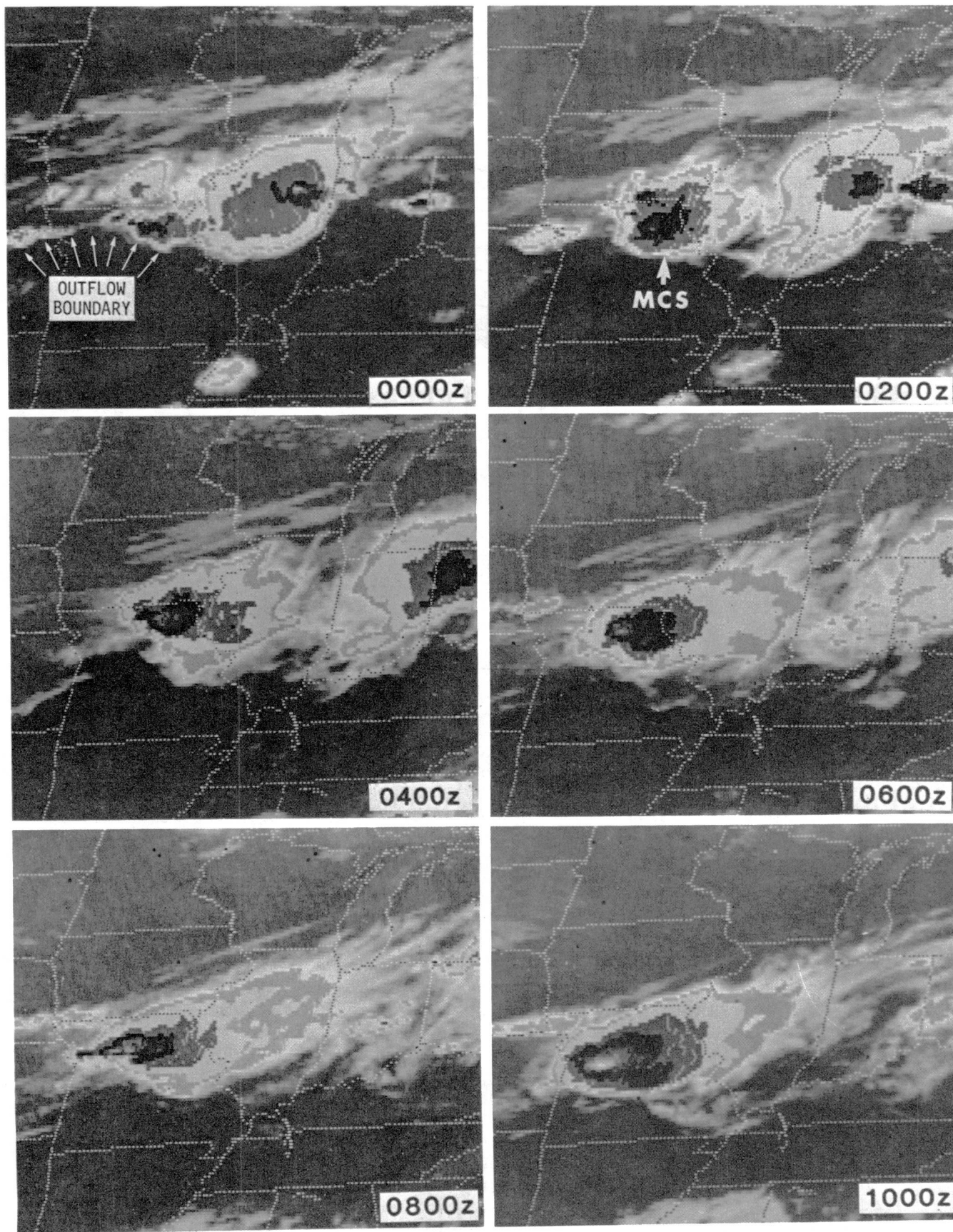


Figure 9a. A backward propagating MCS; enhanced IR imagery (MB Curve), June 25, 1981.

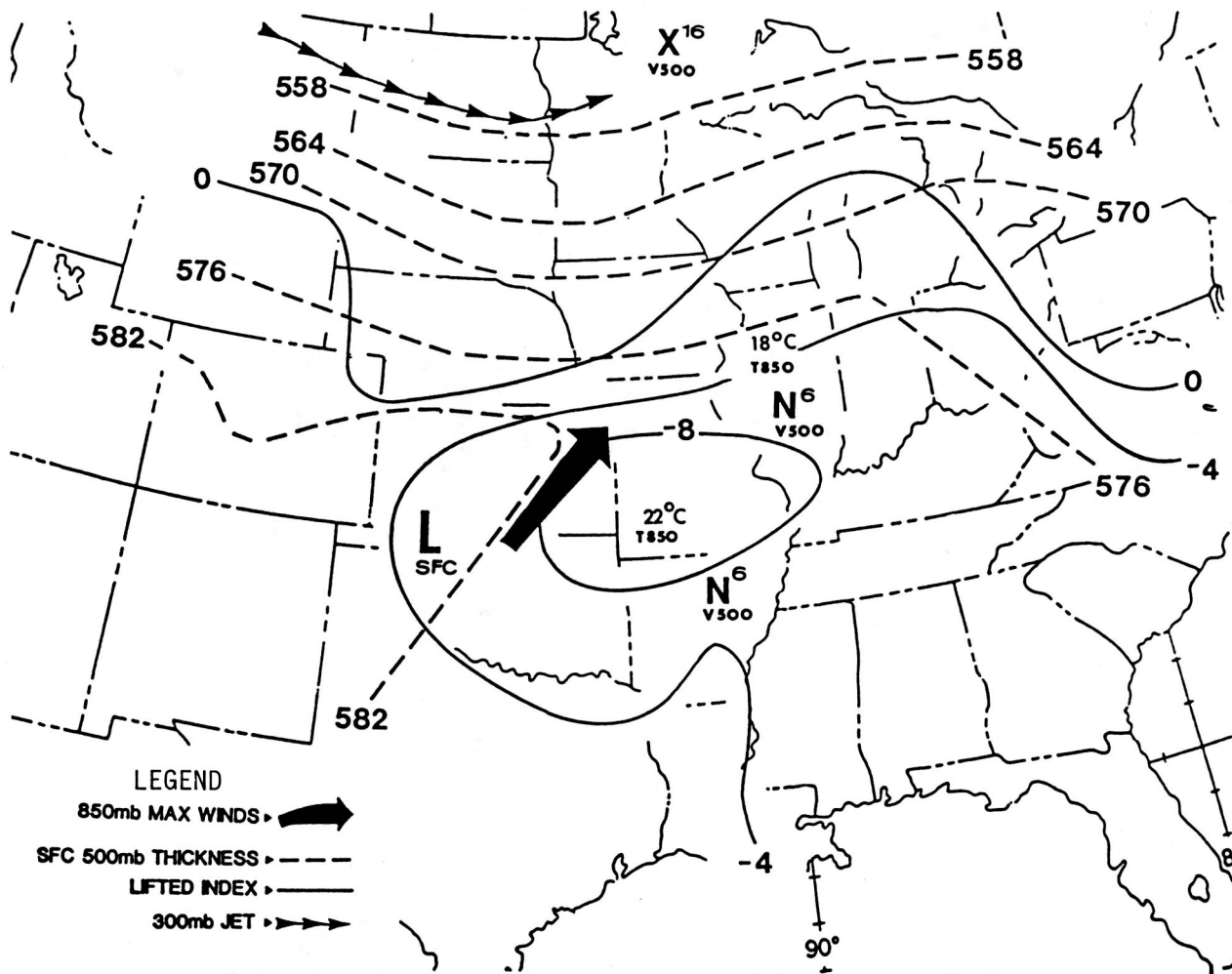


Figure 9b. Surface and upper air features for June 25, 1981, 0000 GMT; T850 indicates 850 mb temperatures in that area and V500 locates either a 500 mb maximum vorticity center (X) or a minimum vorticity center (N). Vorticity values are indicated in 10^{-5} sec^{-1} . Lsfc locates a surface low pressure area.

Backward Propagating MCS (June 25, 1981)

An example of a backward propagating and regenerating MCS is shown in Figures 9a. Accompanying surface and upper air features are shown in Figure 9b. In the imagery, the MCS appears to propagate westward (backward) along an outflow boundary in northern Missouri; the boundary is easier to identify in the late afternoon and evening VIS pictures on the 24th. Other features observed are: a northeast-southwest quasi-stationary front from northern Michigan to Kansas (not shown in Figure 9b), a maximum 850 mb flow of very unstable air into northwest Missouri; no PVA, thickness diffluence, south of an east to west thickness pattern with a moderate gradient and weak upper level winds. Flash flooding occurred with this backward propagating MCS; 5-8 inches of rainfall were reported. In the satellite imagery (Figure 9a), backward propagation is characterized by: (1) an outflow boundary west of the MCS, (2) colder tops occurring in the western portion of the MCS and anvil debris in the eastern portion, (3) small convective cells developing along the outflow boundary to the west of the MCS, and (4) cell mergers along the boundary which in turn merge with the MCS; the result is a westward moving MCS.

V. A SHORT RANGE FORECASTING TECHNIQUE FOR EXPECTED STORM PROPAGATION

It is common for meteorologists to consider the motion of a storm complex as the sum of the mean velocity of the cells comprising the storm complex and the propagation velocity due to new cells forming and accreting to the periphery of the storm. This relationship is illustrated in Figure 10. The mean cell velocity (in Figure 10) may lie along or to either side of the vector mean wind of the cloud layer; propagation may occur anywhere along the storm periphery. If propagation occurs ahead of the storm complex (see forward propagation example in Section IV), an accelerating effect results. If propagation occurs on the rear flank of the storm complex (see backward propagation example in Section IV), a deceleration of the system results.

Newton and Newton (1959) discuss the importance of dynamical interactions between large convective clouds and an environment with wind shear. They show that the total effect of the relative low level inflow into the MCS and the high level outflow from the MCS can be approximated by the vertical wind shear between these two levels. As a result, MCSs often follow a track parallel to the cloud layer shear vector.

Using the above principles, Merritt (1985) and Merritt and Fritsch (1984) studied the movement of mesoscale beta elements (MBEs) embedded in MCCs. MBEs have a spatial scale of 10-100 km and time scale of 1-10 hours. MBEs are identified as radar intensity levels of VIP > 3 on radar summary charts and the coldest cloud tops in the infrared (IR) imagery. In many cases, MBE movement is controlled by the mean cloud layer wind and the propagation of the storm, i.e., the vector of the MBE movement is equal to the vector of the mean wind plus the vector of the storm propagation (see Figure 11). As a result, the MBEs move in the direction of the mean cloud-layer shear vector, coincident with the dashed 850-300 mb thickness contours in Figure 12.

In a study by Scofield and Jiang (1987), animation is used to track the movement and evolution of the coldest satellite observed IR cloud tops embedded within MCSs. The movement of these coldest tops is considered the same as the movement of MBEs. In this study, 19 MCS cases were used. MBE movement (determined from animated imagery) and wind shear in various layers were compared. The results are shown in Table 2. The 850-300 mb thickness contour is the best for forecasting the direction of the MBEs; the surface-700 mb thickness contour was best for forecasting MBE speed.

From the satellite analysis of 36 MCS events, it was determined that Merritt and Fritsch's method was good for forecasting the movement of Type I forward/right movers MCSs. Back or opposite and left movers were not forecast well. Right, left, forward, back or opposite movers refer to the deviation of the storm's movement from the mean tropospheric wind. For Type II (bounded propagation), Merritt and Fritsch's method accurately forecasts forward/right movers that have a separation distance of about 10-20 km between the new cells and the main storm (see Table 1). Again, Type II opposite movers or backward propagating storms and independent MCS mergers cannot be forecasted by Merritt and Fritsch's method. The backward propagating MCSs and their resulting mergers are extremely important as they usually are associated with rainfall that is heavier, lasts longer and covers a bigger area than that associated with a forward propagating system (Simpson and Woodley, 1971 and Woodley and Sax, 1976).

THE COMPARISON BETWEEN MBE'S MOVEMENT AND WIND SHEAR IN A VARIETY OF LAYERS
(19 MCSs)

LAYERS (MB)	MEAN DIFFERENCE BETWEEN THE DIRECTION OF MOVEMENT OF MBEs AND WIND SHEAR (DEGREES)	MEAN DIFFERENCE BETWEEN THE SPEED OF MOVEMENT OF MBEs AND WIND SHEAR (M/S)
850-300	9.6	9.5
700-300	17.6	7.0
850-500	23.8	4.2
700-400	25.3	6.3
500-300	31.8	6.1
850-700	37.5	4.4
700-500	49.4	6.7
SURFACE-700	42.6	3.3

Table 2. The comparison between MBEs movement and wind shear in various layers.

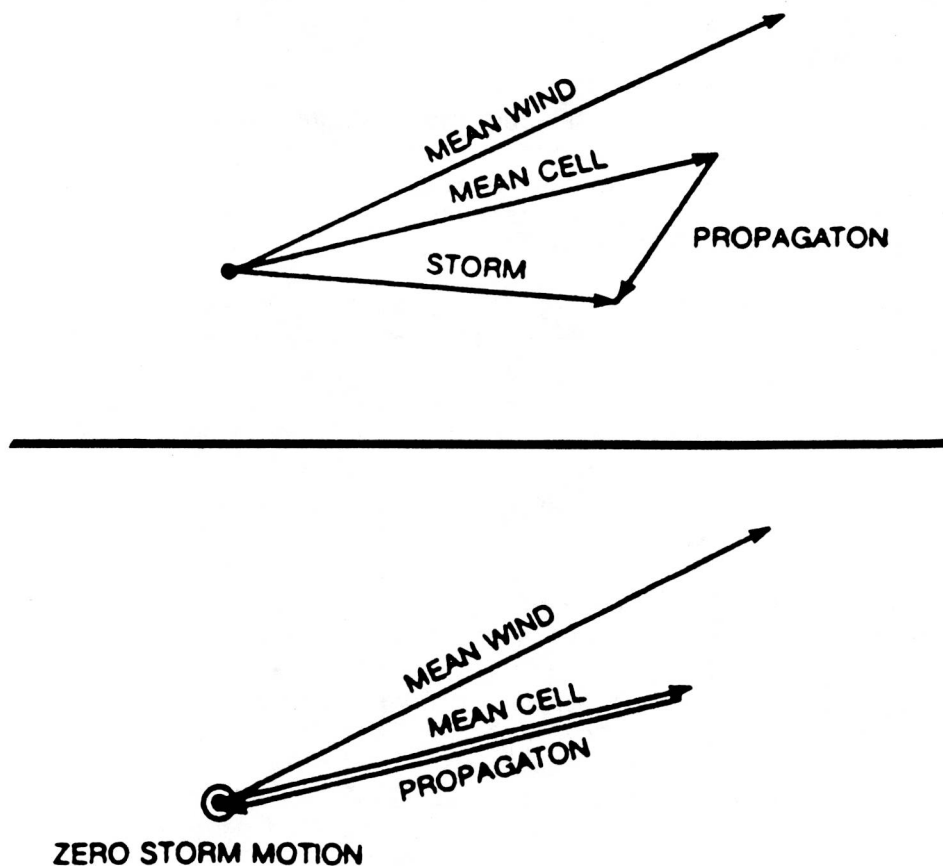


Figure 10. Vector diagram showing the effect of propagation on storm motion (top) and the relationship between propagation and mean cell motion for developing a quasi-stationary MCS (bottom) (from Chappell, 1985).

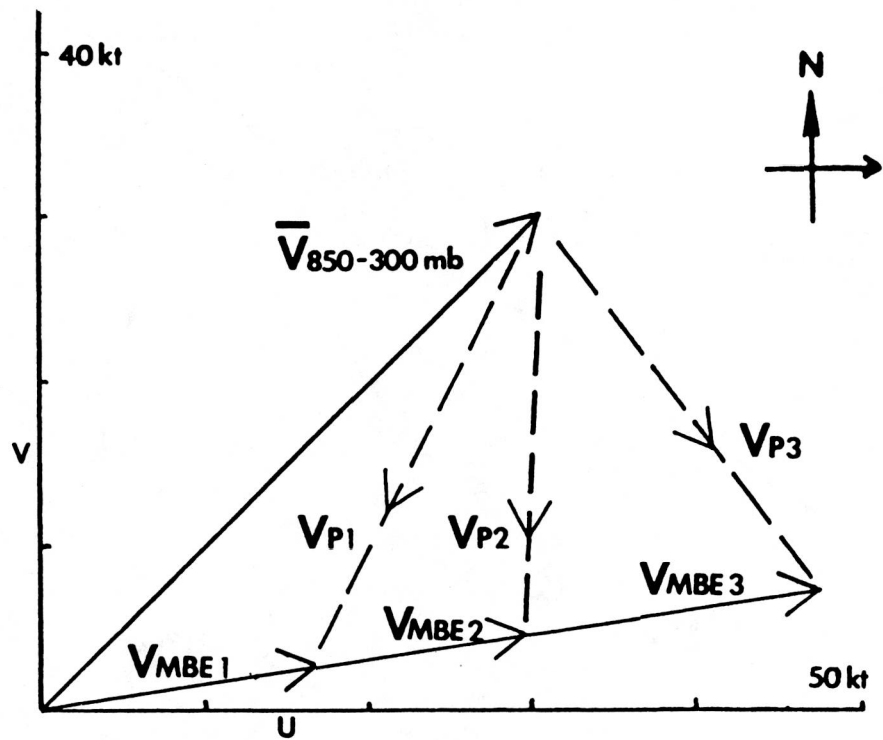


Figure 11. Schematic of the variations of MBE speed as the sum of the mean tropospheric wind, $V_{850-300\text{mb}}$ and storm propagation; V_{MBE} = vector of the MBE movement and V_{p} = vector of the storm propagation (from Merritt and Fritsch, 1984).

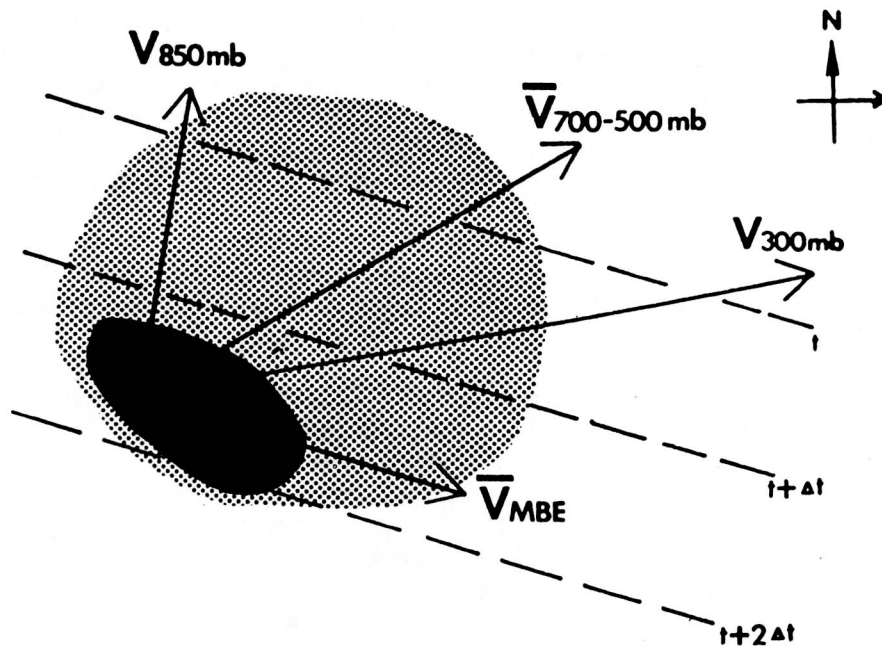


Figure 12. Schematic hodograph showing direction of MBE movement relative to 850 mb and 300 mb wind vectors and the mean mid-tropospheric wind vector ($V_{700-500\text{mb}}$); dashed lines are 850-300 mb thickness contours; light stippling is $<32^{\circ}\text{C}$ cold cloud shield of MCC; dash stippling is region of MBEs (from Merritt and Fritsch, 1984).

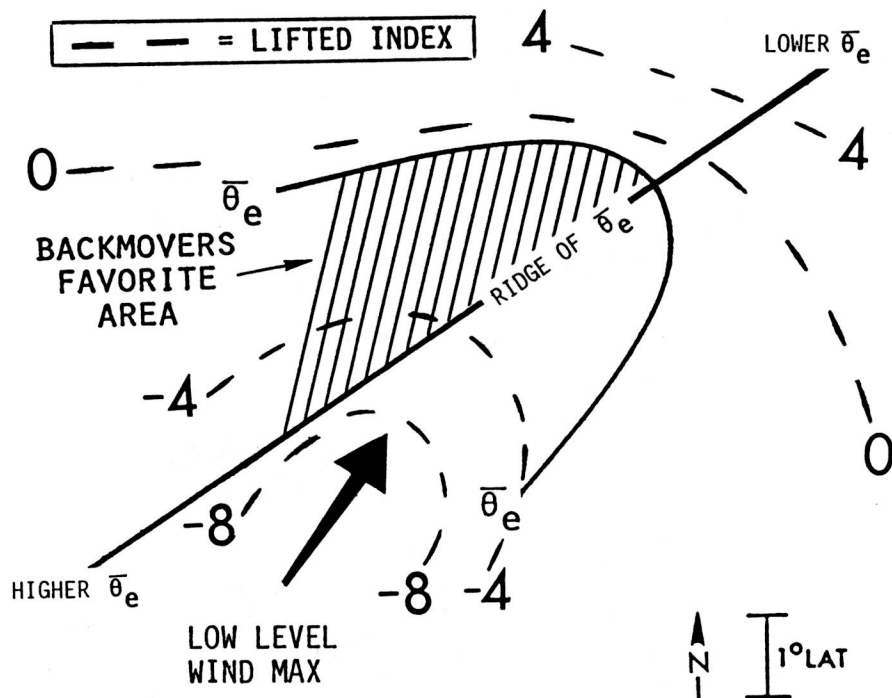


Figure 13. Favorite area (stippled) for the occurrence of backward propagating MCSs; area is located along and north of the mean equivalent potential temperature ($\bar{\theta}_e$) ridge axis.

In this study, 9 backward propagation events are examined in detail. In addition to testing various parameters from Merritt and Fritsch's efforts (1984) mean layer equivalent potential temperature ($\bar{\theta}_e$) is examined for each event. In 8 out of 9 back mover or opposite mover events propagation occurs along the ridge axis of $\bar{\theta}_e$ from low to high values. Backward propagation occurs along and north of the $\bar{\theta}_e$ ridge axis (see Figure 13). The equivalent potential temperature layers of $\bar{\theta}_e$ (300-700 mb) and $\bar{\theta}_e$ (300-850 mb) are best correlated with the backward propagating system; the $\bar{\theta}_e$ are determined from the mandatory levels. Back movers or opposite movers also propagate backward toward higher low level temperatures (surface - 700 mb), lower instability, higher moisture and maximum low level winds (low level jet). Forward propagating systems did not move along the $\bar{\theta}_e$ ridge axis but followed the 850-300 mb thickness isopleths (Merritt and Fritsch's method).

Two examples of backward propagating MCS along or north of the $\bar{\theta}_e$ (300-700mb) axis are shown in Figures 14 and 15. IR imagery for the first example is shown in Figure 6; the MCS propagated backwards along the $\bar{\theta}_e$ axis. The 1000-500 mb thickness (showing diffluence over Oklahoma) and IR imagery for the second example are illustrated in Figures 16, 17a,b, respectively. As observed in Figures 17a and 17b, the MCS propagated backwards and north of the $\bar{\theta}_e$ axis. The position of the $\bar{\theta}_e$ axis was approximately at the same location 12 hours later (June 10, 1200 GMT). Six to eight inches of rain and flash flooding occurred with the backward propagating MCS over northern Oklahoma.

There are cases when a MCS will be a combination of both a forward and backward propagating system. In these situations, the convection associated with the backward propagation is normally dominant and is accompanied by the heaviest rainfall; the forward propagating convection usually weakens with time and dissipates leaving an outflow boundary.

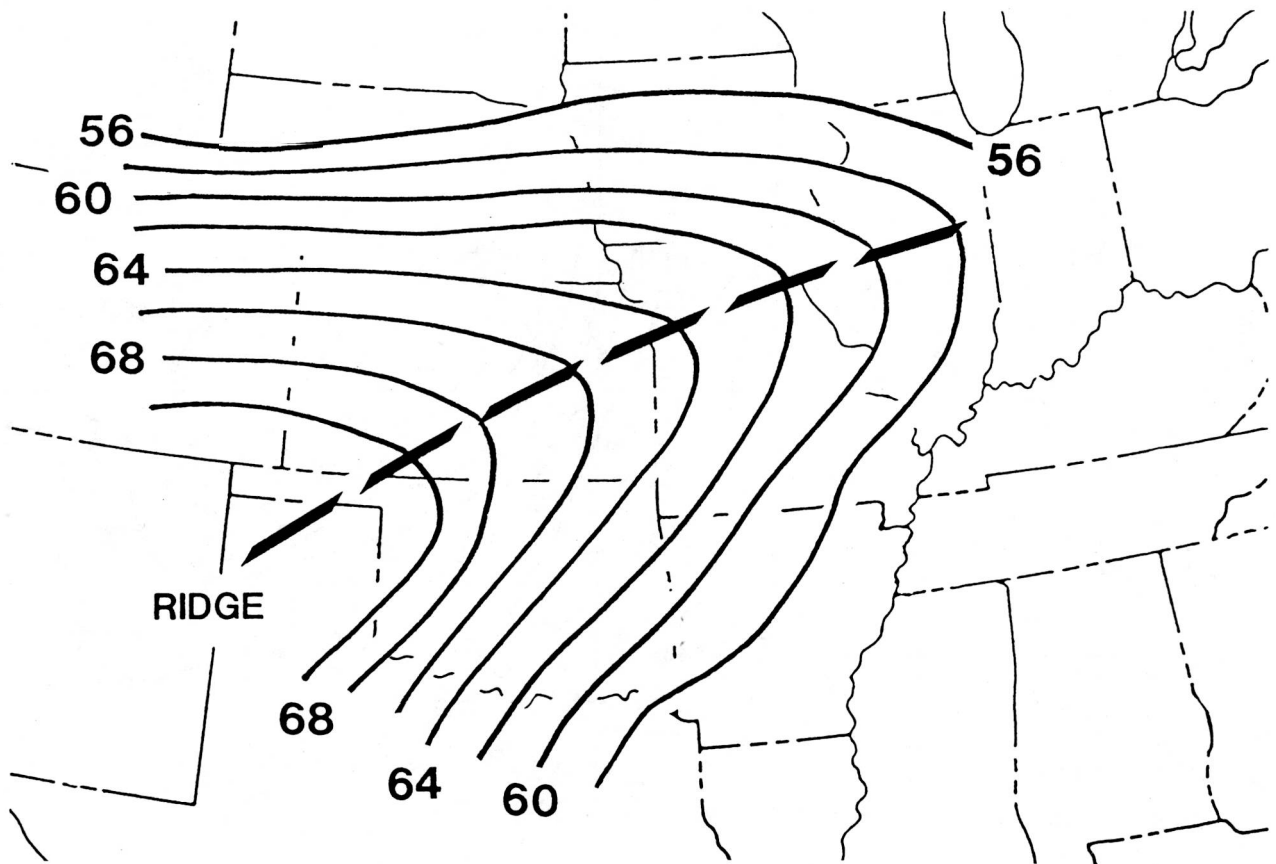


Figure 14. $\bar{\theta}_e$ (300-700mb) analysis ($^{\circ}\text{C}$) for August 4, 1985, 0000 GMT.

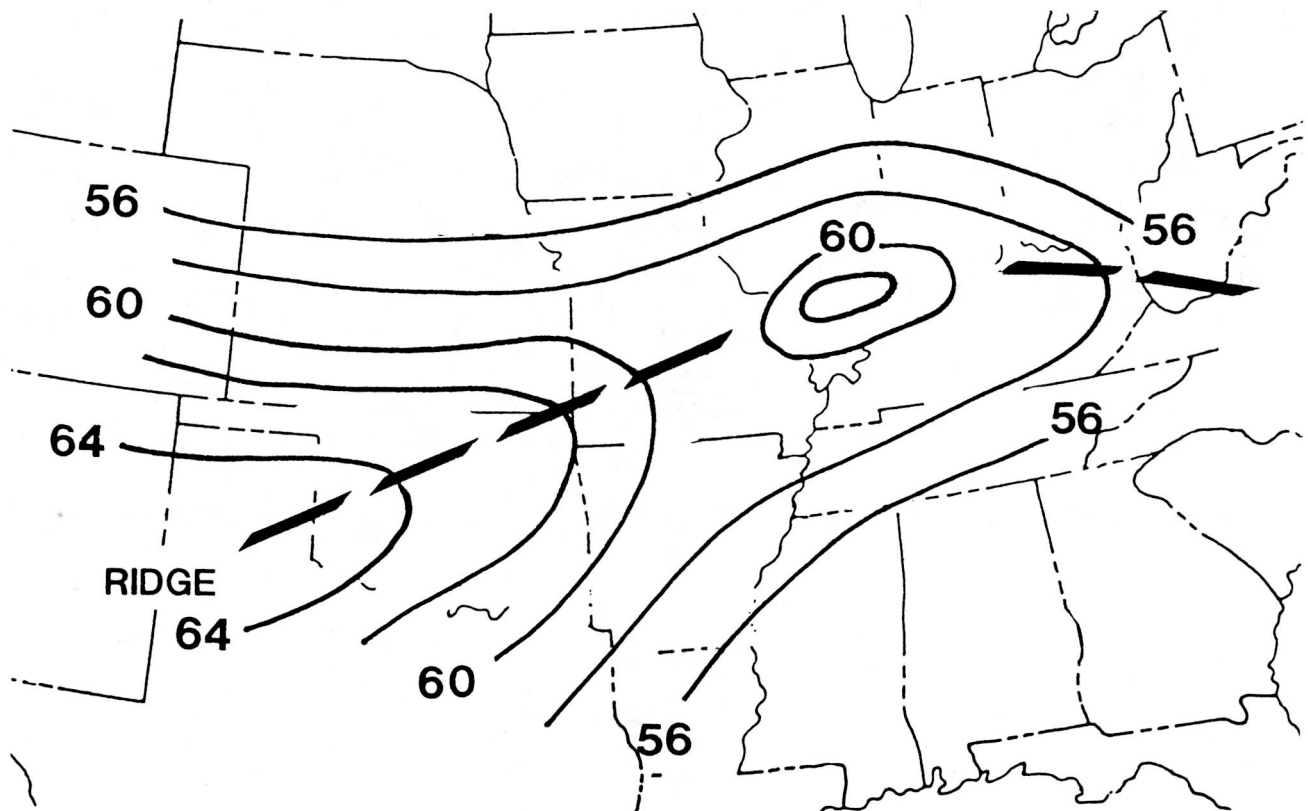


Figure 15. $\bar{\theta}_e$ (300-700mb) analysis ($^{\circ}\text{C}$) for June 10, 1985, 0000 GMT.

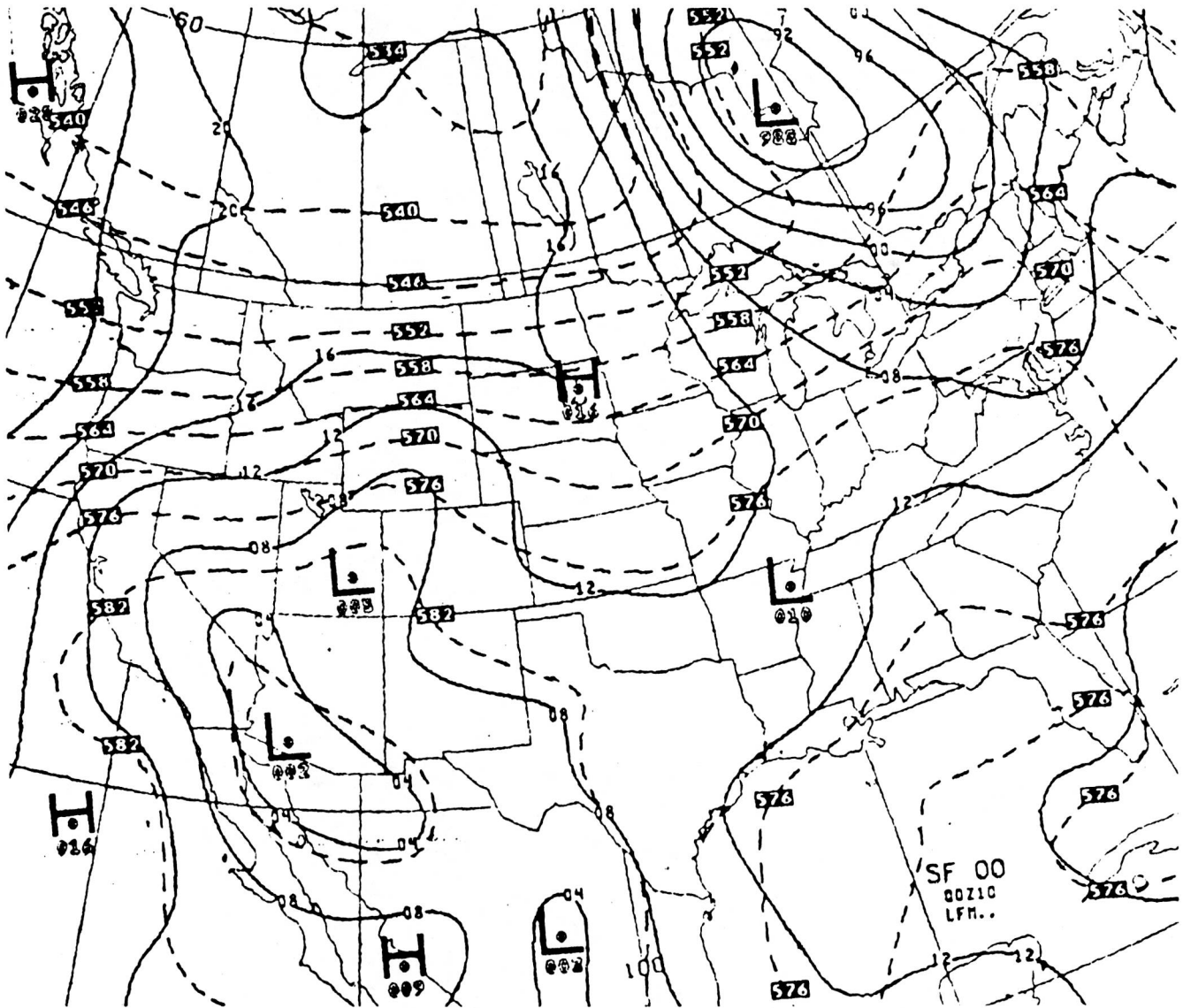


Figure 16. Analysis of surface and 1000-500 mb thickness, 0000 GMT, June 10, 1985.

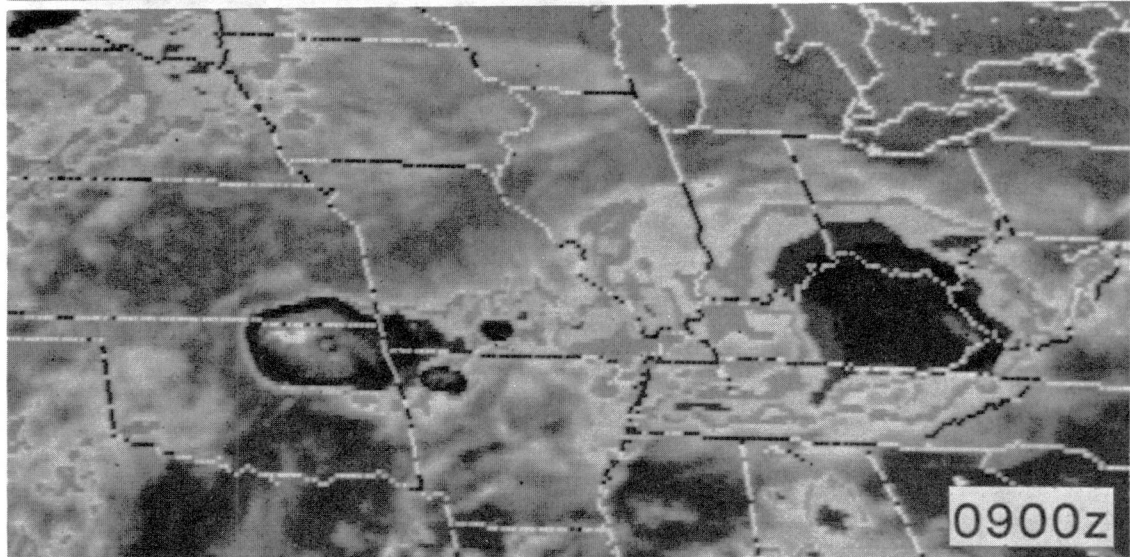
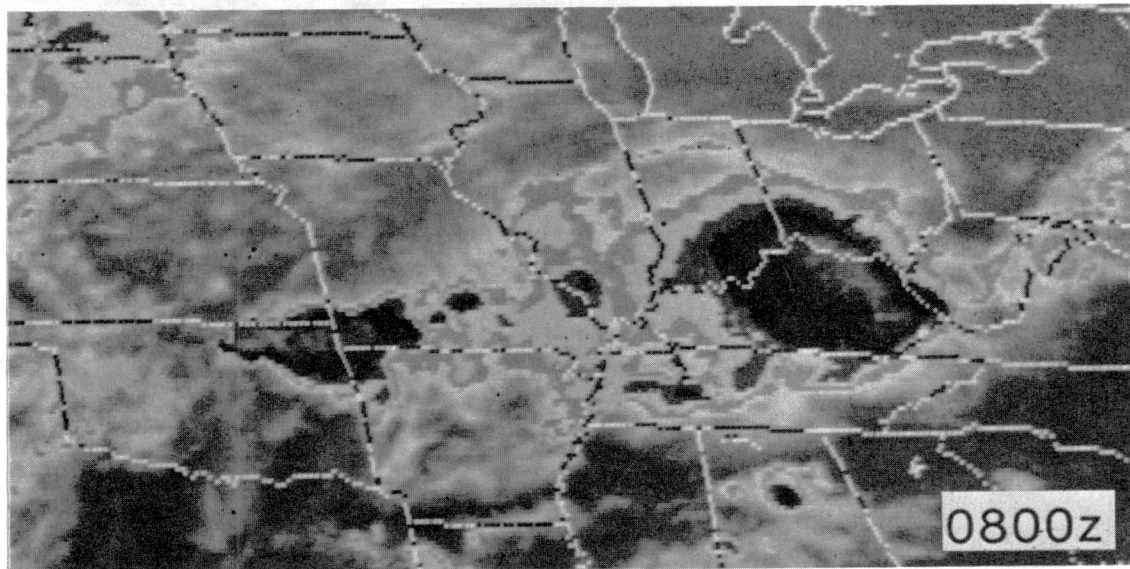
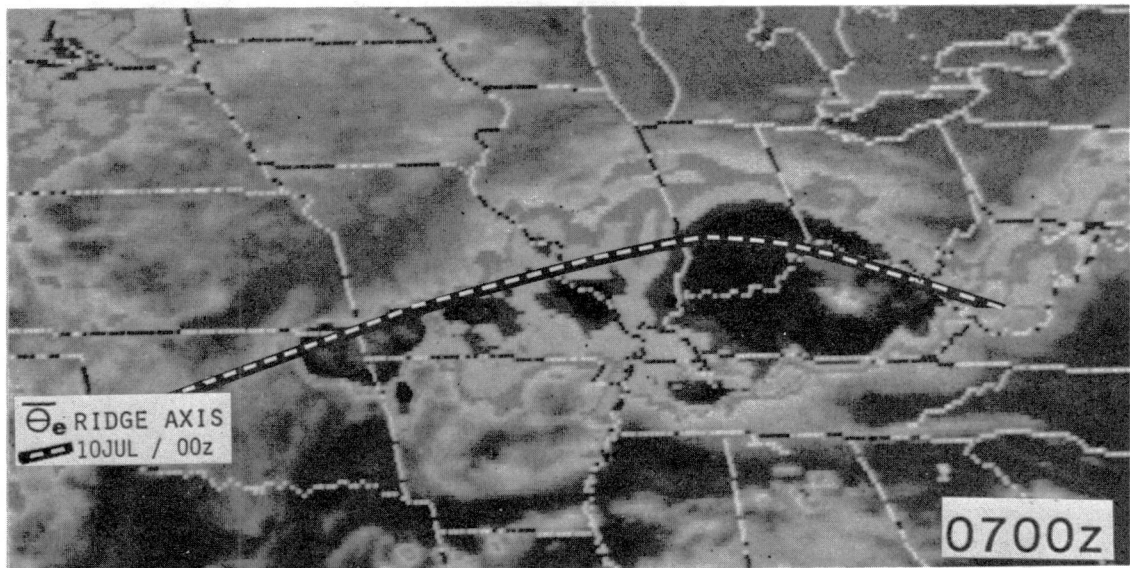


Figure 17a. A backward propagating MCS; enhanced IR imagery (MB Curve), June 10, 1985.

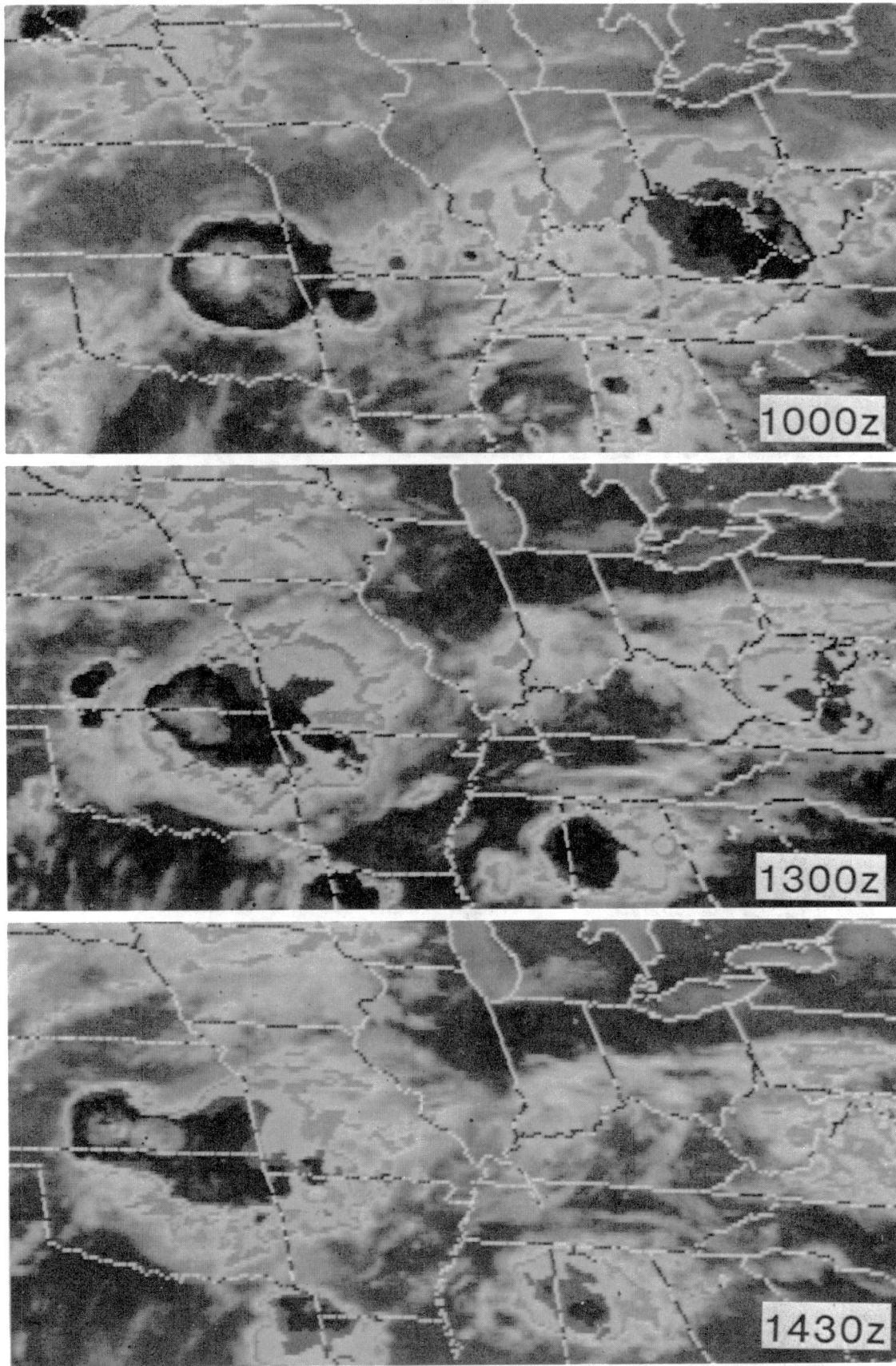


Figure 17b. A backward propagating MCS; enhanced IR imagery (MB Curve), June 10, 1985.

VI. LIFE CYCLE CHARACTERISTICS OF MCSs

The life cycle of MCSs in the satellite imagery is summarized in Table 3; this table and the other information in section 3 were derived from 75 convective events. MCSs evolve in one of six modes: (1) "random" convective elements merging and developing into a MCS, (2) the intersection of two or more lines of convection, (3) a convective line (squall line) transforming into a large, circular- or oval-type of MCS, (4) a cyclonic circulation (MCC or synoptic-scale induced), (5) the remnants of a tropical cyclone, and (6) backward propagation and mergers resulting in large MCSs. A characteristic of some of the mature stages is a tendency for many of the MCSs to regenerate along boundaries. Anticyclonic cirrus outflows and mergers of MBEs are observed with a few of the MCSs. Continuous and bounded propagation are also characteristic of mature stages. Occasionally, some of the circular/oval-type of MCSs split into two separate convective entities before dissipating. Mesoscale-induced jets and mesoscale-induced vortices (Johnston, 1982) are observed with some of the latter stages of the MCS.

Stability is used to describe the thermodynamic structure of the atmosphere. However, an important factor for initiating MCSs is not the existence of instability but the local change of stability with respect to time. The latter factor incorporates both the thermodynamical and dynamical aspects of MCS initiation. The principal stability patterns that initiate MCSs are displayed in Figure 18. In this study (75 cases), the most common type of instability initiation occurred (1) in stability gradients (between lifted index values of -4 and +4) where the low level flow is the strongest and nearly normal to the stability isopleths and when unstable air is advecting into the area; low level warm air advection often accompanies this pattern and (2) near instability minimums (between lifted index values of -4 to -8 or lower) where a significant lobe (at 500 mb) of positive vorticity advection (PVA) and/or a thermal trough is passing over the area. Forecasting MCSs require high density spatial and time resolution data. Hourly, high density surface observations of θ_e were found to be very useful in determining where MCSs will develop and how they will propagate. The following is a list of " θ_e functions" associated with stability decreasing with time and with MCS initiation and propagation: (1) positive advection of θ_e in the lower troposphere, and/or (2) maximum lower tropospheric values of θ_e (along a ridge axis) associated with: surface convergence, PVA at 500 mb, cold air advection at 500 mb and/or maximum temperatures at the surface. Negative stability tendencies can also be computed from the temperature advections differenced between the 500-300 mb layer and the 850-700 mb layer (Barnes, 1987). Cases where instability is not surface based but is found aloft as in regions north of a frontal boundary (overrunning convection) are often located in layers where $\partial\theta_e/\partial z < 0$ (Moore, 1986). Cahir and Lottes (1982) have shown that negative values of the Laplacian of θ_e ($\nabla^2\theta_e < 0$) at the surface located boundaries of maximum θ_e . MCSs often develop where the maximum θ_e boundaries are associated with large and small scale upward vertical motion fields.

Forward and backward propagation, stability and other characteristics of MCSs are summarized in Table 4 and 5, respectively. Forward propagating MCSs have instability present along their leading edge to maintain the convection. In addition, the MCSs are often associated with significant PVA or a thermal trough and they are often embedded in a northwest to southeast thickness pattern (surface to 500 mb) with a weak to moderate thickness gradient and a weak to moderate middle to upper level windflow. Backward propagating MCSs have the following characteristics: (1) maximum 850 mb flow and warm, unstable air are being advected into the area or an area of minimum instability is being lifted by PVA, (2) an outflow or frontal boundary is often present, (3) the existence of thickness diffluence (4) located to the south of an east to west thickness pattern with a weak to moderate thickness gradient and (5) mid to upper level flow is weak.

Backward propagating MCSs usually produce heavier rainfall and more flash floods than forward propagating ones. In both types of propagations, heaviest rainfall occurs for surface to 500 mb precipitable water of ≥ 1.2 inches and relative humidity $\geq 60\%$.

MCSs are called regenerative when two or more unrelated convective systems pass over the same location within a 24 hour period. Regenerating MCSs are different from backward propagating ones and are responsible for many flash floods. An example of a regenerating MCS was the devastating Chicago flash flood of August 14, 1987 (Scofield, 1988). In the satellite imagery regenerative systems are often small, warm top MCSs that propagate forward. The MCSs often develop on a mesoscale or synoptic scale boundary that is detectable in the satellite imagery. Surface and upper air features associated with regenerative systems include: a persistent maximum 850 mb flow of the most unstable air into the area of MCS development (along a boundary), a series of weak 500 mb PVA centers oriented NE-SW over area, a weak thickness gradient, and weak middle to upper level winds.

LIFE CYCLE OF MESOSCALE CONVECTIVE SYSTEMS (MCS)

Stages of
Development

SATELLITE

C
H
A
R
A
C
T
E
R
I
S
T
I
C
S

Initiation

Mature

Dissipation

- | | | |
|--|---|--|
| <ul style="list-style-type: none"> o the merging of random convective elements | <ul style="list-style-type: none"> o a mesoscale convective complex (see Figs. 1a,c) | <ul style="list-style-type: none"> o IR cloud tops warm slowly |
| <ul style="list-style-type: none"> o the intersection of 2 or more linear convective cloud clusters | <ul style="list-style-type: none"> o a multi-clustered circular (see Figs. 1a,c) | <ul style="list-style-type: none"> o IR cloud tops warm rapidly |
| <ul style="list-style-type: none"> o the transformation of a convective line (squall line) | <ul style="list-style-type: none"> o a multi-clustered linear (see Figs. 1a,c) | <ul style="list-style-type: none"> o mesoscale induced vortex |
| <ul style="list-style-type: none"> o the evolution of a cyclonic circulation | <ul style="list-style-type: none"> o a synoptic-scale tropical (see Figs. 1a,c) o a synoptic-scale cyclonic circulation (see Figs. 1a,c) | <ul style="list-style-type: none"> o mesoscale induced jets |
| <ul style="list-style-type: none"> o the remnants of a tropical cyclone circulation | <ul style="list-style-type: none"> o regenerative (see Figs. 1b,c) | <ul style="list-style-type: none"> o a split of the mature system into 2 separate convective entities |
| <ul style="list-style-type: none"> o backward propagation and mergers | <ul style="list-style-type: none"> o anticyclonic outflow o merges within the MBEs o continuous propagation o bounded propagation | |

Table 3. Life Cycle of mesoscale convective systems in the satellite imagery.

FORWARD PROPAGATION, STABILITY AND OTHER CHARACTERISTICS
OF MESOSCALE CONVECTIVE SYSTEMS (MCS)

C
H
A
R
A
C
T
E
R
I
S
T
I
C
S

30

<u>Propagation</u>	<u>Stability</u>	<u>Vertical Motion</u>	<u>Thickness 1000-500 mb</u>	<u>Mid-Upper Level Wind Flow</u>	<u>Moisture</u>
Forward	Max 850 mb flow and unstable air (often parallel to leading edge of MCS)	Significant positive vorticity advection (PVA)	Weak-moderate thickness gradient (usually oriented NW-SE)	Weak-moderate (usually oriented NW-SE)	Sfc-500 mb PW > 1.2 and Sfc-500 mb RH > 60% for heavy rainfall producing storms
	Area of min. instability	Significant PVA and often a 500 mb thermal trough	Weak-moderate thickness gradient (oriented SW-NE E-W or NW-SE)	Weak-moderate (orientations similar to thickness)	
	Max 850 mb flow and unstable air normal to western edge of MCS	PVA center may or may not be present	Thickness diffluence and near to just south of weak-moderate thickness gradient	Near to just south of weak-moderate winds	

Table 4. Forward propagation: Stability, and other characteristics of mesoscale convective systems.

BACKWARD PROPAGATION, STABILITY AND OTHER CHARACTERISTICS
OF MESOSCALE CONVECTIVE SYSTEMS (MCS)

<u>Propagation</u>	<u>Stability</u>	<u>Vertical Motion</u>	<u>Thickness 1000-500 mb</u>	<u>Mid-Upper Level Windflow</u>	<u>Moisture</u>
Backward	Max 850 mb flow and unstable air (often normal to some type of boundary)	Weak	Thickness diffluence south of weak-moderate thickness gradient	Weak; south of stronger winds	Sfc-500 mb PW \geq 1.2 and Sfc-500 mb RH \geq 60% for heavy rainfall producing storms
	Area of min. instability and possibly a boundary present	Weak PVA lobe	Thickness diffluence and/or south of weak-moderate thickness gradient	Weak; south of strong winds	
	Area of min. instability	Significant PVA (or lobe) and/or a 500 mb thermal trough	Near to just south of weak-moderate thickness gradient	Near to just south of stronger winds	

Table 5. Backward propagation: Stability, and other characteristics of mesoscale convective systems.

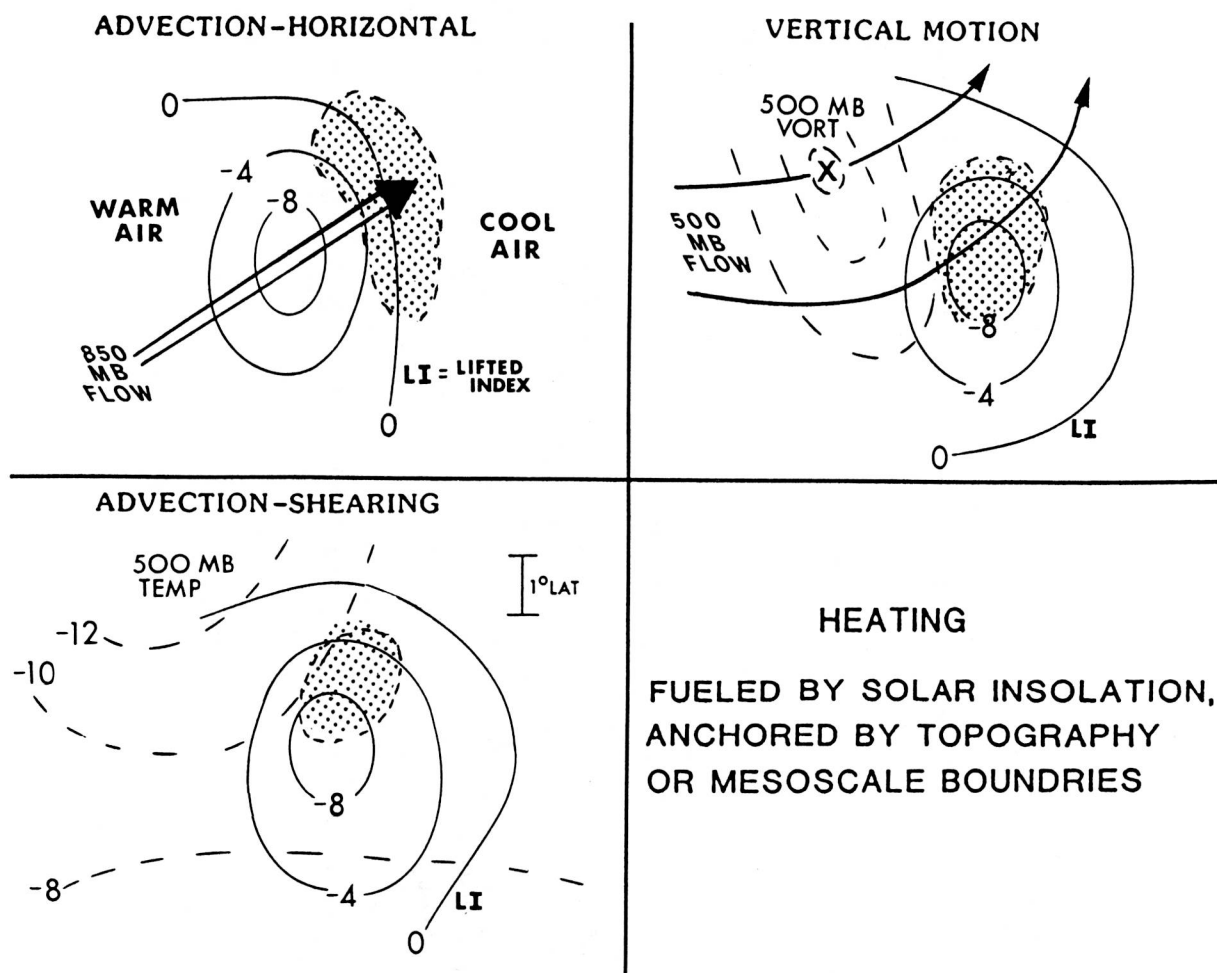


Figure 18. Stability patterns that initiate mesoscale convective systems; stippling represent areas where convection will initiate.

VII. A PROPOSED 3-12 HOUR HEAVY PRECIPITATION FORECAST INDEX (Scofield, 1987)

In order to develop a convective flash flood situation: (1) the atmosphere needs the instability, a boundary and upward vertical motion to develop the thunderstorm, (2) the thunderstorm needs plenty of moisture for it to rain effectively and (3) the thunderstorm needs to propagate or regenerate in such a way that the heavy rain will last more than 1 hour over a particular location. Therefore the ingredients of a 3-12 hour convective heavy precipitation index would include: an instability burst factor (the local change of stability with respect to time - see Figure 18), moisture, storm movement (propagation), boundary and vertical motion considerations. The upward vertical motion must be sufficient to remove any capping inversion or lid (Forbes, et al., 1984). In addition, local forecast office techniques must be used in the decision making process. An example of "local" techniques include: the existence of surface pressure fall centers, preferred thicknesses for heavy rainfall, critical Bulk Richardson Numbers, veering of winds in lower troposphere, etc. (Ray, 1986). As a result of the information compiled and analyzed in this study a preliminary 3-12 hour convective heavy precipitation forecast index is presented.

3-12 HOUR HEAVY PRECIPITATION FORECAST INDEX FOR MCSs

SEE DECISION TREE

3-12 HOUR HEAVY PRECIPITATION FORECAST INDEX
FOR MCSs

Are large scale and small scale upward vertical motion areas present or expected (sufficient to remove any capping inversion or lid)? Use synoptic scale and mesoscale analyses techniques (Ray, 1986). (Includes local forecast office techniques.)

-NO → MCS WILL NOT DEVELOP

YES

Determine if INSTABILITY BURSTS are present or expected

INSTABILITY BURSTS have one or more of the following characteristics

HORIZONTAL ADVECTION

Maximum 850 mb flow normal to Lifted Index (LI) isopleths of -4 to +4; also $(v \cdot \nabla \theta_e)_{sfc} > 0$ which is the positive advection of θ_e at the surface and where v is the horizontal velocity; the advection of θ_e at 850 and 700 mb is also useful; also $\frac{\partial \theta_e}{\partial z} < 0$; $\nabla^2 \theta_e < 0$.

UPWARD VERTICAL MOTION

Significant vertical motion area passing over minimum LI isopleths of -4 to -8 or lower; also $(\theta_{e\max} \nabla \cdot v)_{sfc} < 0$ which is the maximum surface value of θ_e (along the ridge axis) associated with surface convergence and/or $(\theta_{e\max sfc} \nabla \cdot \nabla Q_{500}) > 0$ which is the maximum surface value of θ_e associated with positive absolute vorticity (Q) advection at 500 mb; $\nabla^2 \theta_e < 0$

↓
SHEARING ADVECTION

A thermal trough passing over minimum LI isopleths of -4 to -8 or lower; also $(\theta_{e\max sfc} \cdot \nabla T_{500}) < 0$ which is the maximum surface value of θ_e associated with cold air advection at 500 mb; $\nabla^2 \theta_e < 0$. Also negative stability tendencies computed from the temperature advectations differenced between the 500-300 mb layer and the 850 — 700 mb layer.

↓
HEATING

Fueled by solar insolation, anchored by topography or mesoscale boundaries: LI of +4 or lower, K index of +25 or larger; also $(\theta_{e\max T})_{sfc} > 0$ which is the maximum surface value of θ_e associated with a ridge or area of maximum temperatures at the surface; $\nabla^2 \theta_e < 0$.

↓
ARE INSTABILITY BURSTS
PRESENT OR EXPECTED?

NO → MCS WILL NOT DEVELOP

↓
YES

↓
MCS WILL DEVELOP

↓

WHAT TYPE OF MCS MOVEMENT
IS ANALYZED OR EXPECTED?

↓

BACKWARD PROPAGATING MCS

SATELLITE FEATURES

- o an outflow boundary west of the MCS
- o colder IR tops in western portion of MCS and anvil debris in eastern portion
- o small convective cells along outflow boundary to west of MCS
- o cell mergers along boundary which in turn merge with MCS resulting in a westward moving MCS

SURFACE AND UPPER AIR
FEATURES

- o MCS moves backwards along θ_e ridge axis
 - o MCS moves backwards towards: higher θ_e values, higher temperatures between surface and 700 mb, lower instability, higher moisture and maximum low level winds
 - o thickness diffluence and south of a west to east thickness pattern with a moderate gradient
 - o PVA not normally present
 - o weak upper level winds
 - o veering of winds between surface and 850 mb
- ↓



SLOW FORWARD PROPAGATING MCS

SATELLITE FEATURES

- o a slow eastward (usually southeastward) movement of MCS
- o colder IR tops in western portion of MCS
- o mergers often occur within the MBE

SURFACE AND UPPER AIR FEATURES

- o maximum 850 mb flow maintaining unstable air to western edge of MCS
- o a PVA center may or may not be present
- o thickness diffluence and near to just south of a weak-moderate thickness gradient
- o near to just south of stronger winds aloft
- o a surface boundary may or may not be present
- o MCS moves parallel to 850-300 mb thickness isopleths





REGENERATING MCSs

SATELLITE FEATURES

- o two or more MCSs develop and pass over same location within a 24 hour period
- o MCSs (often small and warm top) move eastward
- o MCSs often develop along a mesoscale or synoptic scale boundary

SURFACE AND UPPER AIR FEATURES

- o a persistent maximum 850 mb flow of the most unstable air into the area of MCS development (along a boundary that is west of flash flood area)
- o several weak 500 mb PVA centers oriented NE-SW over area
- o south of an east to west thickness pattern with a moderate gradient
- o south of the jet stream
- o MCS moves parallel to 850-300 mb thickness and/or θ_e ridge axis
- o weak middle to upper level winds
- o a weak surface boundary





FAST FORWARD PROPAGATING MCS

SATELLITE FEATURES

- o a rapid eastward (usually southeastward) movement of MCS
- o colder IR tops in eastern portion of MCS
- o mergers not usually detected

SURFACE AND UPPER AIR FEATURES

- o maximum 850 mb flow maintaining unstable air to leading edge of MCS
- o a PVA center present
- o northwest-southeast thickness isopleths present with a moderate gradient
- o MCS moves parallel to 850-300 mb thickness isopleths
- o a moderate to strong upper level flow pattern just north of area
- o a surface boundary may or may not be present



IS A BACKWARD PROPAGATING, SLOW FORWARD PROPAGATING OR REGENERATING MCSs ANALYZED OR EXPECTED?

NO → MCS WILL MOVE TOO FAST TO PRODUCE HEAVY PRECIPITATION AND FLASH FLOODS.

YES



↓
HOW MUCH MOISTURE IS AVAIL-
ABLE OR EXPECTED?

↓
CRITERIA FOR MCS TO PRODUCE
HEAVY PRECIPITATION

- o sfc - 500 mb precipitable water of > 1.2 inches
- o sfc - 500 mb relative humidity of > 60%
- o sfc dewpoint ridge or area of > 60°F
- o sfc mixing ratio ridge
- o sfc (or 850 mb) moisture convergence
- o positive advection of sfc dewpoints
or mixing ratios

↓
ARE MOST OR ALL OF THE
ABOVE CRITERIA PRESENT
OR EXPECTED?

→ NO → TOO DRY TO PRODUCE
HEAVY PRECIPITATION
AND FLASH FLOODS.

↓
YES

↓
HEAVY PRECIPITATION
AND
FLASH FLOODS
ARE EXPECTED

↓
END OF TECHNIQUE

VIII. SUMMARY AND OUTLOOK

This study discusses MCS propagation characteristics. Two types of satellite propagation are identified: Type I - Continuous or Type II - Bounded. Type I propagation are usually forward or right movers. Forward propagating MCSs often move parallel to the 850-300 mb thickness isopleths. Type II propagations are normally backward or opposite movers. Backward propagating MCS are often associated with strong mergers that result in prolonged heavy rainfall and flash floods. Backward or opposite movers frequently occur along the $\bar{\theta}_e$ (300-700 mb or 300-850 mb) ridge axis and propagate backward towards higher $\bar{\theta}_e$ values, higher low level temperatures, lower instability, higher moisture and maximum low level winds. Regenerating MCSs are different from backward propagating ones and are responsible for many flash floods.

The ingredients for a 3-12 hour convective heavy precipitation index include: an instability burst factor (the local change of stability with respect to time), available moisture, type of MCS propagation and location of the large scale and small scale upwind vertical motion areas. The positive advection of θ_e and the maximum surface values of θ_e associated with surface convergence proved to be most useful in determining where MCSs will develop and propagate. In the future, the convective available potential energy (Moncrieff and Miller, 1976) will be used as the stability parameter in the instability burst factor. Differential thickness advection will be further examined as an indicator of MCS development. The Laplacian of θ_e will be tested as a "tool" for locating boundaries that may initiate MCSs.

Obviously more MCS events must be studied in order to better understand their propagation characteristics. Three to fifteen minute interval satellite data is needed to study the propagation characteristics of MCSs; this data is available and will be used in future investigations. In the near future, GOES-VIS and IR spin scan radiometer atmospheric sounder (VAS) sounding data will be available on the VAS Data Utilization Center (VDUC) system. As a result, GOES VAS-derived moisture, stability, low level winds, θ_e , thickness fields, and other products will be a better source of data to study the satellite propagation and stability characteristics of MCSs. Thus planned future efforts will involve archiving convective events and performing analyses on the VDUC system. The use of VDUC for analyzing and forecasting heavy rainfall producing MCSs is presented in a paper by Scofield (1988).

Additional efforts will consider a similar methodology taking parameters that evolve from this study and future ones and apply them to extratropical cyclones and tropical systems. Initial studies on the stability characteristics of extratropical cyclones indicate that instability bursts and conditional symmetric instability (CSI) (Bennetts and Sharp, 1982) may be important mechanisms in the production of heavy "winter storm" precipitation. CSI may also play an important role in tropical cyclones and MCSs.

IX. ACKNOWLEDGMENTS

The authors thank Frances Holt and Andy Timchalk of the Satellite Applications Laboratory of NESDIS for their constructive criticism in the preparation of this manuscript, Tina Cashman for typing, John Shadid and Gene Dunlap for the preparation of illustrations and layout.

X. REFERENCES

- Barnes, S. L., 1987: Analysis of quasi-geostrophic forcing during the AIMCS project. NOAA Tech Memo ERL ESG-27, Vol. I, Boulder.
- Bennetts, D. A., and J. C. Sharp, 1982: The relevance of conditional symmetric instability to the production of mesoscale frontal rainbands. Quart. J. Roy. Meteor. Soc., 108, 595-602.
- Brooks, H. B., 1946: A summary of some radar thunderstorm observations. Bull. Amer. Meteor. Soc., 27, 557-563.
- Browning, K. A., 1964: Airflow and precipitation trajectories within severe local storms which travel to the right of the winds. J. Atmos. Sci., 21, 634-639.
- Cahir, J. J. and W. D. Lottes, 1982: An objective diagnostic aid in locating meteorologically significant boundaries. Preprints, 9th Conf. on Wea. Fore. and Anal., Seattle, WA, Amer. Meteor. Soc., 296-299.
- Chappell, C. F., 1985: Requisite conditions for the generation of stationary thunderstorm systems having attendant excessive rains. Preprints, 6th Conf. on Hydrometeor., Indiannapolis, IN, Amer. Meteor. Soc., 221-225.
- Chappell, C. F., 1986: Quasi-stationary convective events. Chapter 13 (pp. 289-305) of Mesoscale Meteorology and Forecasting, editor Peter Ray, Amer. Meteor. Soc., Boston, 793 pp.
- Doswell, C. A., 1985: The operational meteorology of convective weather. Volume II: Storm Scale Analysis. NOAA Tech. Memo ERL ESG-15, Boulder.
- Fleming, E. L. and L. E. Spayd, Jr., 1986: Characteristics of western region flash flood events in GOES imagery and conventional data. NOAA Tech. Memo NESDIS 13, Washington, DC.
- Forbes, G. S., P. O. G. Heppner, J. J. Cahir, and W. D. Lottes, 1984: Prediction of delayed-onset nocturnal convection based on air trajectories. Preprints, 10th Conf. on Wea. Fore. and Anal., Clearwater Beach, FL, Amer. Meteor. Soc., 474-479.

- Johnston, E. C., 1982: Mesoscale vorticity centers induced by mesoscale convective complexes. Preprints, 9th Conf. on Wea. Fore. and Anal., Seattle, WA, Amer. Meteor. Soc., 196-200.
- Maddox, R. A., 1980: Mesoscale convective complexes. Bull. Amer. Meteor. Soc., 61, 1374-1387.
- Merritt, J. H., 1985: The synoptic environment and movement of mesoscale convective complexes over the United States. Masters Thesis, Pennsylvania State University, 129 pp.
- Merritt, J. H. and J. Michael Fritsch, 1984: On the movement of the heavy precipitation areas of mid-latitude mesoscale convective complexes. Preprints, 10th Conf. on Wea. Fore. and Anal., Clearwater Beach, FL, Amer. Meteor. Soc., 529-536.
- Moncrieff, M. W. and M. J. Miller, 1976: The dynamics and simulation of tropical cumulonimbus and squall lines. Quart. J. Roy. Meteor. Soc., 102, 373-394.
- Moore, J. T., 1986: On the forecasting of thunderstorms using convective instability. Submitted for publication in Weather and Forecasting (AMS).
- Newton, C. W. and J. C. Fankhauser, 1975: Movement and propagation of multicellular convective storms. Pure Appl. Geophys., 113, 747-764.
- Newton, C. W. and H. R. Newton, 1959: Dynamical interactions between large convective clouds and environment with vertical shear. J. Meteor., 16, 483-496.
- Ray, P. S., 1986: Editor of Mesoscale Meteorology and Forecasting, Amer. Meteor. Soc., Boston, 793 pp.
- Scofield, R. A. and Jiang Shi, 1987: Evolutionary characteristics of mesoscale convective systems and extratropical cyclones observed through satellite animation and conventional data. Proceedings, Workshop on Satellite (and Radar) Imagery Interpretation, Bracknell, UK.
- Scofield, R. A., 1985: Satellite convective categories associated with heavy precipitation. Preprints, 6th Conf. on Hydrometeor., Indianapolis, IN, Amer. Meteor. Soc., 42-51.
- Scofield, R. A., 1987: Ingredients for a short range forecasting heavy precipitation index. Preprints, 7th Conf. on Hydrometeor., Edmonton, Alta., Canada, Amer. Meteor. Soc.
- Scofield, R. A., 1988: Using the VAS Data Utilization Center (VDUC) for the analysis and forecasting of heavy rainfall producing Mesoscale Convective Systems (MCSs). Preprints, 3rd Conf. on Satellite Meteor. and Oceanography, Anaheim, CA, Amer. Meteor. Soc.
- Simpson, J. and W. L. Woodley, 1971: Seeding cumulus in Florida: New 1970 results. Science, 172, 117-126.

Wilhelmson, R. B. and C. S. Chen, 1982: Simulations of the development of successive cells along a cold outflow boundary. J. Atmos. Sci., 39, 1456-1465.

Woodley, W. L. and R. I. Sax, 1976: The Florida area cumulus experiment: rationale, design, procedures, results and future course. NOAA Tech. Rept. ERL 354-WMP06, Miami.

(Continued from inside front cover)

- NESDIS 8 A Technique that Uses Satellite, Radar, and Conventional Data for Analyzing and Short-Range Forecasting of Precipitation from Extratropical Cyclones. Roderick A. Scofield and Leroy E. Spayd Jr., November 1984. (PB85 164994/AS)
- NESDIS 9 Surface Cyclogenesis as Indicated by Satellite Imagery. Frank Smigielski and Gary Ellrod, March 1985. (PB85 191815/AS)
- NESDIS 10 Detection of High Level Turbulence Using Satellite Imagery and Upper Air Data. Gary Ellrod, April 1985. (PB85 208452/AS)
- NESDIS 11 Publications and Final Reports on Contracts and Grants, 1984. Nancy Everson, April 1985. (PB85 208460/AS)
- NESDIS 12 Monthly Infrared Imagery Enhancement Curves: A Tool for Nighttime Sea Fog Identification off the New England Coast. E.M. Maturi and Susan J. Holmes, May 1985. (PB85 237725/AS)
- NESDIS 13 Characteristics of Western Region Flash Flood Events in GOES Imagery and Conventional Data. Eric Fleming and Leroy Spayd Jr., May 1986. (PB86 209459/AS)
- NESDIS 14 Publications and Final Reports on Contracts and Grants, 1985. Nancy Everson, June 1986. (PB86 232477/AS)
- NESDIS 15 An Experimental Technique for Producing Moisture Corrected Imagery from 1 Km Advanced Very High Resolution Radiometer (AVHRR) Data. Eileen Maturi, John Pritchard and Pablo Clemente-Colon, June 1986. (PB86 24535/AS)
- NESDIS 16 A Description of Prediction Errors Associated with the T-Bus-4 Navigation Message and a Corrective Procedure. Frederick W. Nagle, July 1986. (PB87 195913)
- NESDIS 17 Publications and Final Reports on Contracts and Grants, 1986. Nancy Everson, April 1987. (PB87 220810/AS)
- NESDIS 18 Tropical Cyclone Center Locations from Enhanced Infrared Satellite Imagery. J. Jixi, and V.F. Dorvak, May 1987. (PB87 213450/AS)
- NESDIS 19 A Suggested Hurricane Operational Scenario for GOES I-M. W. Paul Menzel, Robert T. Merrill and William E. Shenk, July 1987. in press

NOAA SCIENTIFIC AND TECHNICAL PUBLICATIONS

The National Oceanic and Atmospheric Administration was established as part of the Department of Commerce on October 3, 1970. The mission responsibilities of NOAA are to assess the socioeconomic impact of natural and technological changes in the environment and to monitor and predict the state of the solid Earth, the oceans and their living resources, the atmosphere, and the space environment of the Earth.

The major components of NOAA regularly produce various types of scientific and technical information in the following kinds of publications:

PROFESSIONAL PAPERS—Important definitive research results, major techniques, and special investigations.

CONTRACT AND GRANT REPORTS—Reports prepared by contractors or grantees under NOAA sponsorship.

ATLAS—Presentation of analyzed data generally in the form of maps showing distribution of rainfall, chemical and physical conditions of oceans and atmosphere, distribution of fishes and marine mammals, ionospheric conditions, etc.

TECHNICAL SERVICE PUBLICATIONS—Reports containing data, observations, instructions, etc. A partial listing includes data serials; prediction and outlook periodicals; technical manuals, training papers, planning reports, and information serials; and miscellaneous technical publications.

TECHNICAL REPORTS—Journal quality with extensive details, mathematical developments, or data listings.

TECHNICAL MEMORANDUMS—Reports of preliminary, partial, or negative research or technology results, interim instructions, and the like.



U.S. DEPARTMENT OF COMMERCE
NATIONAL OCEANIC AND ATMOSPHERIC ADMINISTRATION
NATIONAL ENVIRONMENTAL SATELLITE, DATA, AND INFORMATION SERVICE
Washington, D.C. 20233